



Ghent University

Faculty of Engineering

Department of Flow, Heat and Combustion

Academic Year 2015-2016

**Development of a simplified sensitivity analysis approach to quantify life safety for risk assessment of buildings in case of fire**

José Morales

Promoter: Bart Merci

Co-promotor: Bart Van Weyenberge

Master thesis submitted in the Erasmus Mundus Study Programme

**International Master of Science in Fire Safety Engineering**

This thesis is submitted in partial fulfilment of the requirements for the degree of *The International Master of Science in Fire Safety Engineering (IMFSE)*. This thesis has never been submitted for any degree or examination to any other University/programme. The author declares that this thesis is original work except where stated. This declaration constitutes an assertion that full and accurate references and citations have been included for all material, directly included and indirectly contributing to the thesis. The author gives permission to make this master thesis available for consultation and to copy parts of this master thesis for personal use. In the case of any other use, the limitations of the copyright have to be respected, in particular with regard to the obligation to state expressly the source when quoting results from this master thesis. The thesis supervisor must be informed when data or results are used.

A handwritten signature in black ink, appearing to read 'Jose', with a large, stylized flourish above it and a long horizontal line extending to the right.

José Fernando Morales

30 April 2016 Read and approved

## **ABSTRACT**

The present thesis is elaborated as an extension to the research presented by Bart Van Weyenberge in his PHD thesis “Sensitivity analysis for QRA of life safety in case of fire”.

Performing fire safety designs based on performance criteria traditionally relies on deterministic analyses to describe the risk levels for a predetermined fire scenario. The problem in this matter lies in the high number of variables involving a risk scenario that may be overlooked by deterministic analyses. Therefore risk-informed methods based on probabilities are the next step in order to deal with these uncertainties. The preceding sensitivity analysis plays a significant role reducing the number of variables allowing to make an accurate first guess of the risk presented by the design.

This thesis investigates two methods of performing sensitivity analyses. The objective is to better understand the most significant input parameters in case of fire, evaluating life safety risk in basis of temperature, visibility and toxicity. The parameters of study are those related to the physical properties of fuel packages. 360 fire simulations divided are carried out each representing differences either in geometry, conditions within the enclosure and location of the fire source. 2 different fire simulation models are employed to execute the simulations, namely CFD and CFAST. The results of the simulations are then evaluated by 2 sensitivity methods, the Elementary Effect method (Morris method) and by estimating the global level of sensitivity index of the input parameters.

## **ABSTRACTO**

La presente tesis es elaborada como una extensión a la investigación presentada por Bart Van Weyenberge en sus trabajos de doctorado “Análisis de sensibilidad para QRA de riesgo a la vida en caso de incendios”.

Diseños de seguridad en caso de incendios basados en desempeño tradicionalmente han confiado en análisis deterministas para describir el nivel de riesgo en caso de incendios. El problema para este tipo de diseños es en alto número de variables relacionados con los escenarios de riesgo que pueden ser ignorados por los análisis deterministas. Por esta razón métodos de análisis de riesgo basados en probabilidades parece ser un acercamiento más apropiado. El análisis de sensibilidad previo desempeña un papel importante reduciendo el número de variables permitiendo realizar una precisa primera aproximación del riesgo presentado por el diseño.

La presente tesis sugiere la implementación de dos tipos de análisis de sensibilidad. El objetivo es entender de una mejor forma los parámetros de entrada en caso de incendios, evaluando el riesgo de vida en base a temperatura, visibilidad y niveles tóxicos. 360 simulaciones de fuego son realizados, cada uno presentando diferencias ya sea en geometría, condiciones dentro del recinto y ubicación de la fuente de fuego. 2 diferentes tipos de modelos de simulación de fuegos son utilizados para llevar a cabo las simulaciones, estos son CFD y CFAST. Los resultados de las simulaciones son entonces evaluados por dos métodos de análisis de sensibilidad, el método de Elementos Elementales (método de Morris) y por medio de la estimación del nivel global del índice de sensibilidad de los parámetros de entrada.

## Table of contents

ABSTRACT.....	ii
ABSTRACTO .....	iii
List of Abbreviations .....	vii
List of figures.....	ix
List of tables .....	xi
1. Introduction .....	1
2. Literature review.....	3
2.1. Risk .....	3
2.1.1. Definition of Risk .....	3
2.1.2. Risk Management .....	4
2.2. Risk Assessment .....	5
2.3. Risk Analysis .....	6
2.3.1. Values/Objectives: .....	6
2.3.2. System Models:.....	6
2.3.3. Risk scenarios:.....	6
2.3.4. Likelihood and consequences: .....	7
2.3.5. Qualitative risk assessment: .....	7
2.3.6. Semi-quantitative risk assessment: .....	8
2.4. Quantitative risk assessment .....	8
2.4.1. Frequentistic or deterministic point of view.....	9
2.4.2. The subjective or Bayesian point of view .....	9
2.5. Risk presentation and risk evaluation.....	10
2.5.1. Risk matrix.....	10
2.5.2. FN – curves.....	11
2.6. Fire risk assessment .....	12
2.7. Life safety criteria.....	13
2.7.1. Thermal injuries. ....	13
2.7.2. Toxicity. ....	13
2.7.3. Reduction of visibility.....	14
2.8. Fire Computer Models .....	16
2.8.1. Definition of fire computer models. ....	16
2.8.2. Zone models.....	16

2.8.3.	CFD .....	18
2.9.	Sensitivity analysis .....	21
2.9.1.	Definition of sensitivity analysis.....	21
2.10.	Sensitivity Analysis methods.....	21
3.	Case Study .....	29
3.1.	Approach .....	29
3.2.	Setup .....	33
3.2.1.	Case 1: Retail shop .....	33
3.2.2.	Case 2: Bar.....	35
3.2.3.	Case 3: Bar with sprinkler system .....	36
3.2.4.	Case 4: Bar with extraction system.....	38
3.2.5.	Case 5: Bar ventilation-controlled fire .....	39
4.	Results and discussion .....	40
4.1.	Case 1: Retail shop .....	41
4.1.1.	Resulting $\mu^*$ and $\sigma$ at main exit .....	41
4.1.2.	Total sensitivity index results at main exit.....	42
4.2.	Case 2: Bar .....	43
4.2.1.	Resulting $\mu^*$ and $\sigma$ at main exit .....	43
4.2.2.	Total sensitivity index results at main exit:.....	44
4.3.	Case 3: Bar with sprinkler system .....	45
4.3.1.	Resulting $\mu^*$ and $\sigma$ at main exit .....	45
4.3.2.	Total sensitivity index results at main exit.....	46
4.4.	Case 4: Bar with extraction system.....	47
4.4.1.	Resulting $\mu^*$ and $\sigma$ at main exit .....	47
4.4.2.	Total sensitivity index results at main exit.....	48
4.5.	Case 5: Bar ventilation-controlled fire .....	49
4.5.1.	Resulting $\mu^*$ and $\sigma$ at main exit .....	49
4.5.2.	Total sensitivity index results at main exit.....	50
5.	Conclusions .....	51
6.	SUGGESTIONS .....	52
7.	Acknowledgements.....	53
8.	References.....	54
	APPENDIX A.....	57

APPENDIX B..... 59  
APPENDIX C..... 64

## List of Abbreviations

R	Risk
S	Possible risk scenario
P	Probability of occurrence
X	Consequence/Input parameter/sample values
ISO	International Organization for Standardization
FTA	Fault tree
ETA	Event tree
QRA	Quantitative Risk Assessment
PBD	Performance Based Design
NFPA	National Fire Protection Association
NIST	National Institute of Standards and Technology
RSET	Required Safe Egress Time
ASET	Available Safe Egress Time
$C_s$	Smoke extinction coefficient
FED	Fractional Effective Dose
FEC	Fractional Effective Concentration
EE	Elementary Effect
$\mu$	Mean
$\mu^*$	Mean of absolute values
$\sigma$	Standard deviation
$\alpha$	Growth rate of fire
HOC	Heat of Combustion
HRR	Heat Release Rate
$\dot{Q}$	Heat Release Rate
HRRPUA	Heat Release Per Unit Area
QR	Quasi Random
kW	kiloWatt
m	meter
kJ/kg	kiloJoule/kilogram
g/g	gram/gram
Ao	Area of opening
Ho	Height of opening
$\Omega$	K-Dimensional Unit Cube (standardized)
k	Number of input factors
r	Number of points
$\Delta$	Predetermined multiple of $1/(p-1)$



p	Levels for calculation
B*	Matrix with dimensions $(k+1) \times k$
J $_{k+1,1}$	$(k+1) \times k$ Matrix of 1's and x*
D*	K-Dimensional diagonal Matrix
F <sub>i</sub>	Distribution of elementary effects
G <sub>i</sub>	Distribution of the absolute values of the elementary
ST <sub>i</sub>	Total Sensitivity Index
V(Y)	Variance of Variable Y
CFD	Computer Fluid Dynamics
FDS	Fire Dynamics Simulator
CFAST	Consolidated Model of Fire Growth and Smoke Transport
SHC	Smoke and Heat Control
LES	Large Eddy Simulation
UQLab	Uncertainty Quantification Laboratory

## List of figures

FIGURE 1: ACTIVITIES OF THE RISK MANAGEMENT PROCESS .....	4
FIGURE 2: RISK ASSESSMENT PROCESS .....	5
FIGURE 3: CONCEPT OF BOW-TIE MODEL .....	7
FIGURE 4: RISK MATRIX .....	10
FIGURE 5: FN – CURVE FOR SOCIETAL RISK.....	11
FIGURE 6: COMPARISON OF INTERNATIONAL STANDARDS IN FN FORMAT.....	11
FIGURE 7: WALKING SPEED IN FIRE SMOKE.....	14
FIGURE 8: EXAMPLE OF A TRAJECTORY IN THE INPUT SPACE WHEN $K=3$ , USING POINTS (1,1,2) AS BASE POINTS .....	22
FIGURE 9: OPTIMIZED TRAJECTORY WITH ALL POSSIBLE COMBINATIONS (LEFT) TRAJECTORIES PUSHED TO THE OUTSIDE (RIGHT) OPTIMIZED TRAJECTORIES WITH SECOND CRITERION ( $P=4, R=4$ & $M=6$ ).....	24
FIGURE 10: ORIGINAL SAMPLING STRATEGY (LEFT) AND IMPROVED STRATEGY (RIGHT).....	24
FIGURE 11: EXAMPLE OF A RADIAL TRAJECTORY IN THE INPUT SPACE WHEN $K=3$ , USING POINTS (1,1,2) AS BASE POINTS.	26
FIGURE 12: ENERGY RELEASE RATES FOR DIFFERENT GROWTH RATES.....	31
FIGURE 13: RETAIL SHOP LAYOUT.....	33
FIGURE 14: RETAIL SHOP FDS LAYOUT AND LOCATION OF DEVICES .....	34
FIGURE 15: FDS BAR LAYOUT AND DEVICES LOCATION.....	35
FIGURE 16: SPRINKLER LOCATION ACCORDING TO [32].....	37
FIGURE 17: EXTRACTION VENT DISTRIBUTION.....	38
FIGURE 18: VENTILATION-CONTROLLED FIRE.....	39
FIGURE 19: COLOR IDENTIFICATION OF PARAMETERS.....	40
FIGURE 20: TIME AVERAGES.....	40
FIGURE 21: FDS RESULTS CASE 1. TEMPERATURE MAIN EXIT .....	41
FIGURE 22: CFAST RESULTS CASE 1. TEMPERATURE MAIN EXIT .....	41
FIGURE 23: FDS RESULTS CASE 1. CO LEVELS MAIN EXIT .....	42
FIGURE 24: CFAST RESULTS CASE 1. CO LEVELS MAIN EXIT UPPER LAYER .....	42
FIGURE 25: FDS RESULTS CASE 2. TEMPERATURE MAIN EXIT .....	43
FIGURE 26: CFAST RESULTS CASE 2. TEMPERATURE MAIN EXIT .....	43
FIGURE 27: FDS RESULTS CASE 2. CO LEVELS MAIN EXIT .....	44
FIGURE 28: CFAST RESULTS CASE 2. CO LEVELS MAIN EXIT UPPER LAYER .....	44
FIGURE 29: FDS RESULTS CASE 3. TEMPERATURE MAIN EXIT .....	45
FIGURE 30: CFAST RESULTS CASE 3. TEMPERATURE MAIN EXIT.....	45
FIGURE 31: FDS RESULTS CASE 3. CO LEVELS MAIN EXIT .....	46
FIGURE 32: CFAST RESULTS CASE 3. CO LEVELS MAIN EXIT UPPER LAYER .....	46
FIGURE 33: FDS RESULTS CASE 4. TEMPERATURE MAIN EXIT .....	47
FIGURE 34: CFAST RESULTS CASE 4. TEMPERATURE MAIN EXIT .....	47
FIGURE 35: FDS RESULTS CASE 4. CO LEVELS MAIN EXIT .....	47
FIGURE 36: CFAST RESULTS CASE 4. CO LEVELS MAIN EXIT UPPER LAYER .....	47
FIGURE 37: FDS RESULTS CASE 5. TEMPERATURE MAIN EXIT .....	49
FIGURE 38: CFAST RESULTS CASE 5. TEMPERATURE MAIN EXIT .....	49
FIGURE 39: FDS RESULTS CASE 5. CO LEVELS MAIN EXIT .....	50
FIGURE 40: CFAST RESULTS CASE 5. CO LEVELS MAIN EXIT UPPER LAYER .....	50

FIGURE C.1.1: FDS RESULTS CASE 1. TEMPERATURE EXIT 1 .....	64
FIGURE C.1.2: FDS RESULTS CASE 1. CO LEVELS EXIT 1 .....	64
FIGURE C.1.3: CFAST RESULTS CASE 1. TEMPERATURE EXIT 1 .....	64
FIGURE C.1.4: CFAST RESULTS CASE 1. CO LEVELS EXIT 1 UPPER LAYER .....	64
FIGURE C.3.1: FDS RESULTS CASE 2. TEMPERATURE EXIT 1 .....	65
FIGURE C.3.2: FDS RESULTS CASE 2. CO LEVELS EXIT 1 .....	65
FIGURE C.3.3: CFAST RESULTS CASE 2. TEMPERATURE EXIT 1 .....	65
FIGURE C.3.4: CFAST RESULTS CASE 2. CO LEVELS EXIT 1 UPPER LAYER .....	65
FIGURE C.5.1: FDS RESULTS CASE 3. TEMPERATURE EXIT 1 .....	66
FIGURE C.5.2: FDS RESULTS CASE 3. CO LEVELS EXIT 1 .....	66
FIGURE C.5.3: CFAST RESULTS CASE 3. TEMPERATURE EXIT 1 .....	66
FIGURE C.5.4: CFAST RESULTS CASE 3. CO LEVELS EXIT 1 UPPER LAYER .....	66
FIGURE C.7.1: FDS RESULTS CASE 4. TEMPERATURE EXIT 1 .....	68
FIGURE C.7.2: FDS RESULTS CASE 4. CO LEVELS EXIT 1 .....	68
FIGURE C.7.3: CFAST RESULTS CASE 4. TEMPERATURE EXIT 1 .....	68
FIGURE C.7.4: CFAST RESULTS CASE 4. CO LEVELS EXIT 1 UPPER LAYER .....	68
FIGURE C.9.1: FDS RESULTS CASE 5. TEMPERATURE EXIT 1 .....	69
FIGURE C.9.2: FDS RESULTS CASE 5. CO LEVELS EXIT 1 .....	69
FIGURE C.9.3: CFAST RESULTS CASE 5. TEMPERATURE EXIT 1 .....	69
FIGURE C.9.4: CFAST RESULTS CASE 5. CO LEVELS EXIT 1 UPPER LAYER .....	69

## List of tables

TABLE 1: CRITICAL CONDITIONS IN FIRE ENCLOSURES .....	15
TABLE 2. ENCLOSURE ZONE FIRE MODELS .....	17
TABLE 3. CFD FIRE MODELS .....	19
TABLE 4: FIVE-DIMENSIONAL SOBOLE QUASI-RANDOM SEQUENCE, FIRST FIVE POINTS. NORMALIZED VALUES [0,1] .....	27
TABLE 5: SOBOLE QUASI-RANDOM SEQUENCE AND RADIAL TRAJECTORIES.....	27
TABLE 6: RANGE OF VALUES OF INPUT PARAMETERS.....	30
TABLE 7: MEAN AND STANDARD DEVIATION FOR INPUT PARAMETERS.....	30
TABLE 8: VALUES OF A FOR DIFFERENT GROWTH RATES .....	31
TABLE 9: EXIT DIMENSIONS .....	34
TABLE 10: EXITS AND OPENING DIMENSIONS.....	35
TABLE 11: GROWTH RATE VALUES AND ACTIVATION TIMES FOR SPRINKLER SYSTEM .....	36
TABLE 12: INPUT VALUES FOR CFD CALCULATIONS OF ACTIVATION TIMES FOR SPRINKLERS .....	37
TABLE 13: GROWTH RATE VALUES AND ACTIVATION TIMES FOR EXTRACTION SYSTEM.....	38
TABLE 14: FDS RESULTS CASE 1. TOTAL SENSITIVITY INDEX MAIN EXIT .....	42
TABLE 15: CFAST RESULTS CASE 1. TOTAL SENSITIVITY INDEX MAIN EXIT .....	42
TABLE 16: FDS RESULTS CASE 2. TOTAL SENSITIVITY INDEX MAIN EXIT .....	44
TABLE 17: CFAST RESULTS CASE 2. TOTAL SENSITIVITY INDEX MAIN EXIT .....	44
TABLE 18: FDS RESULTS CASE 3. TOTAL SENSITIVITY INDEX MAIN EXIT .....	46
TABLE 19: CFAST RESULTS CASE 3. TOTAL SENSITIVITY INDEX MAIN EXIT .....	46
TABLE 20: FDS RESULTS CASE 4. TOTAL SENSITIVITY INDEX TEMPERATURE MAIN EXIT .....	48
TABLE 21: CFAST RESULTS CASE 4. TOTAL SENSITIVITY INDEX TEMPERATURE MAIN EXIT .....	48
TABLE 22: FDS RESULTS CASE 5. TOTAL SENSITIVITY INDEX MAIN EXIT .....	50
TABLE 23: CFAST RESULTS CASE 5. TOTAL SENSITIVITY INDEX MAIN EXIT .....	50
TABLE A.1 RESULTS A 0.04. BAR MAIN EXIT.....	57
TABLE A.2 RESULTS A 0.04. BAR EXIT 1 .....	57
TABLE A.3 RESULTS A 0.08. BAR MAIN EXIT .....	57
TABLE A.4 RESULTS A 0.08. BAR EXIT 1 .....	58
TABLE A.5 RESULTS A 0.12. BAR MAIN EXIT .....	58
TABLE A.6 RESULTS A 0.12. BAR EXIT 1 .....	58
TABLE B.1: RESULTING MATRIX FROM SOBOLE SEQUENCE FOR CASE 1: RETAIL SHOP.....	60
TABLE B.2: RESULTING MATRIX FROM SOBOLE SEQUENCE FOR CASE 2 AND 4: BAR AND BAR WITH EXTRACTION SYSTEM ....	61
TABLE B.3: RESULTING MATRIX FROM SOBOLE SEQUENCE FOR CASE 3: BAR WITH SPRINKLER SYSTEM .....	62
TABLE B.4: RESULTING MATRIX FROM SOBOLE SEQUENCE FOR CASE 4: BAR VENTILATION-CONTROLLED FIRE .....	63
TABLE C.2.1: FDS RESULTS CASE 1. TOTAL SENSITIVITY INDEX EXIT 2 .....	64
TABLE C.2.2: CFAST RESULTS CASE 1. TOTAL SENSITIVITY INDEX EXIT 2 .....	65
TABLE C.4.1: FDS RESULTS CASE 2. TOTAL SENSITIVITY INDEX EXIT 1 .....	66
TABLE C.4.2: CFAST RESULTS CASE 2. TOTAL SENSITIVITY INDEX EXIT 1 .....	66
TABLE C.6.1: FDS RESULTS CASE 3. TOTAL SENSITIVITY INDEX EXIT 1 .....	67
TABLE C.6.2: CFAST RESULTS CASE 3. TOTAL SENSITIVITY INDEX EXIT 1 .....	67
TABLE C.8.1: FDS RESULTS CASE 4. TOTAL SENSITIVITY INDEX EXIT 1 .....	68
TABLE C.8.2: CFAST RESULTS CASE 4. TOTAL SENSITIVITY INDEX EXIT 1 .....	69
TABLE C.10.1: FDS RESULTS CASE 5. TOTAL SENSITIVITY INDEX EXIT 1 .....	70

TABLE C.10. 2: CFAST RESULTS CASE 5. TOTAL SENSITIVITY INDEX EXIT 1..... 70

## 1. Introduction

Traditionally fire safety design has relied on a set of criteria and regulations set by international standards or codes, such as the NFPA, that provides guidance to achieve what would be considered as an acceptable fire safety design applicable to any type of building. These “specifications” includes type of construction materials, water flows for sprinklers and hydrants, distance between sprinklers, to mention a few.

While these specifications have been proven effective over the years, it is rather general providing guidance for what would be considered as common building geometries and processes not addressing complex buildings resulting in unnecessary and expensive installation of systems or construction materials. This drives engineers to an alternative method known as Performance Based Design which is the use of engineering tools and expert judgement to design and develop arrangements for, but not limited to, facilities with unique features or special operation systems providing equal or better level of protection in comparison with the prescription design. PBD is never an easy task and requires a deep understanding of the fire phenomena in order to comply with the stakeholders requirements and to be accepted by the authorities having jurisdiction. According to [1] PBD is defined as an engineering approach to fire protection design based on:

1. Agreed upon fire safety goals and objectives.
2. Deterministic and/or probabilistic analysis of fire scenarios.
3. Quantitative risk assessment of designs alternatives against the fire safety goals and objectives using accepted engineering tools, methodologies and performance criteria.

The objective of this framework lies in point number 2 of the PBD definition. Deterministic approaches are considered a fine solution for a fire safety design, basing the analysis on experimental correlations and/or statistic from literature studies, arriving to a “worst case scenario”. However it holds a fundamental problem which is the high number of variables that are not taken into account, leaving the possibility that an even worst case hasn’t been studied or experimented on yet. For this reason a probabilistic approach seems more appropriate allowing the designer to analyze as many scenarios as desired. Nonetheless this produces another problem, how do we define how much is enough? There are endless possible variables to choose from. Which variables are considered as the most important to take into consideration?

The goal of this thesis is to be able to determine and understand the most important parameters for life safety in case of fire to reduce the dimensionality of the problem. To do so a literature review of the risk assessment process, CFD modelling and Sensitivity Analysis methods employed for the research are provided in section 2 followed by an extensive sensitivity analysis study of different case scenarios arriving to results that will allow, as previously stated, the identification of the most important parameters in case of fire for life safety.

## 2. Literature review

### 2.1. Risk

#### 2.1.1. Definition of Risk

There is no universal definition of risk, however it is associated with a wide range of definitions that varies according to the observer interpretations, associations, beliefs. Some definitions are: actions or inactions that resulted in consequences, risk is equal to expected loss, a combination between hazard and vulnerability... It does not matter how it is defined, one thing is certain: risk is unavoidable, it is inherently attached to our daily life, we must identify and accept a certain level of risk. How to define this acceptable level is a complex process requiring the evaluation and judgement of the task at hand. This is known as risk analysis, the most broadly accepted definition of risk analysis was proposed by [2] which consist in three questions denominated as "Set of Triplets Idea":

- What can happen?
- How likely is it to happen?
- What are the consequences?

Or presented in a mathematical form:

$$R = \{(S, P, X)\} \quad (1)$$

Where:

$R$  = risk

$S$  = possible risk scenario.

$P$  = probability of occurrence for that scenario. Either deterministic or probabilistic.

$X$  = consequences.

Risk analysis is concerned with answering these questions.



Important definitions involving the risk phenomena:

- Individual risk: Expected number of fatalities or injuries to which a specific person is exposed in a year.
- Societal risk: Probability of fatalities or injuries of a large quantity of people from a single catastrophic accident.
- Acceptable risk: A level of risk that is accepted even when the consequences are known e.g. driving a car.
- Tolerable risk: A tolerable level of risk when certain benefits are derived from it.
- ALARP (as low as reasonably practicable): An acceptable level of risk taking into consideration the cost benefit of the scenario.

### 2.1.2. Risk Management

Risk management is defined as the creation and evaluation of options for initiating or changing human activities or structures with the objective of increasing the net benefit to human society and preventing harm to humans and what they value; the implementation of chosen options and the monitoring of their effectiveness [3].

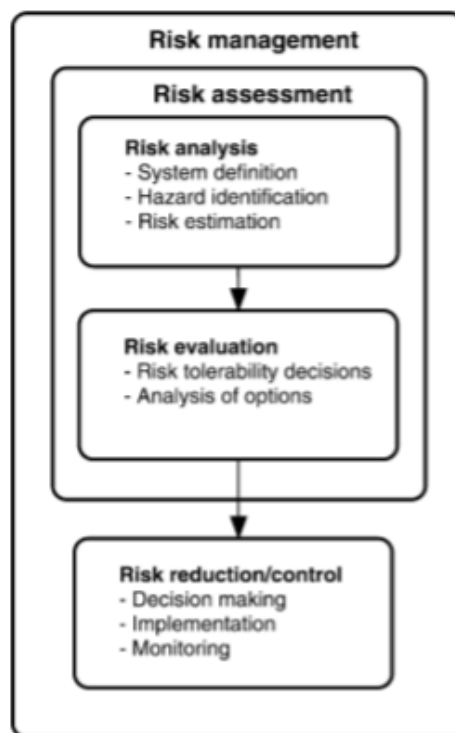


Figure 1: Activities of the risk management process. From [4]

Risk management is in other words all the activities and processes that provides foundation to control risk. Our daily life is controlled by risk management with all the small decisions and implications that they carry. An example of risk management:

It's a snowy day and there are three transport options to arrive at a certain destination:

- Walk.
- Ride a bicycle.
- Ride a car.

There is no right answer, only decisions that may bring more benefit at a higher risk, although riding a bicycle would probably be the least appropriate, a simple risk assessment should be made considering all the aspects regarding the situation, i.e. the severity of the snow, if the road are frozen, the time disposal, and according to a quick risk/benefit evaluation a decision is made.

## 2.2. Risk Assessment

ISO defines it as the overall process of risk identification, risk analysis and risk evaluation [5]. Risk assessment is one part of the risk management process.

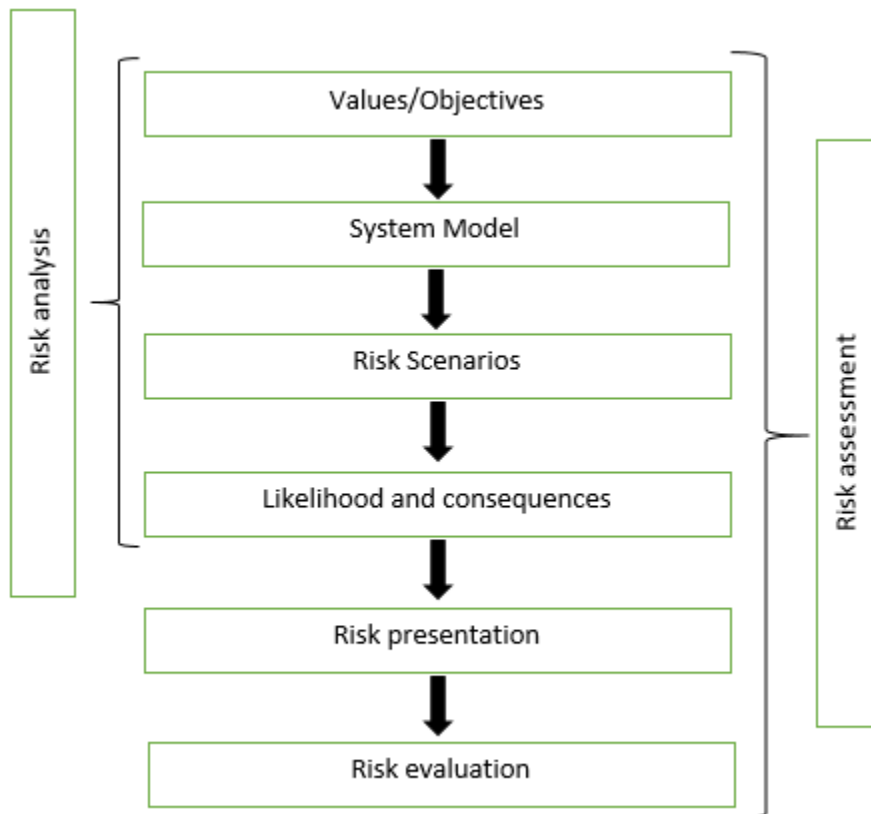


Figure 2: Risk Assessment process. Adapted from [6]

The basic idea of risk assessment is not to try to present all (which is unrealistic) the different types of risk assessment methods that are available but rather to provide a general framework which can be used in combination with many different methods [7]. Risk assessment can be presented in different ways according to the purpose and the depth of the analysis carried out and can be classified as: qualitative, semi-quantitative and quantitative risk assessment discussed in sections 2.4 and 2.5.

## **2.3. Risk Analysis**

Risk analysis provides an input to risk evaluation and to decisions on whether the risk needs to be treated, and on the most appropriate risk treatment and methods [5]. Risk analysis is a part of the risk assessment process, composed of:

### **2.3.1. Values/Objectives:**

What would be considered important for the stakeholders and what they are interested in protecting, e.g. when analyzing a shopping mall it is of great interest the conservation of life within the enclosure, while a production center of any kind of goods might also be interested in business continuity since delays, even just days, may cause considerable monetary losses.

### **2.3.2. System Models:**

Description of the systems or context of the design from which the risk scenarios are originated. The level of detail of the description of a given scenario must be expressed in the same manner when describing the consequences, e.g. if the consequences are described in terms of number of fatalities then it also must be shown the estimated number of people present when the scenario was initiated.

### **2.3.3. Risk scenarios:**

Description of the possible scenarios or sequence of events leading to negative consequences. Fault and event trees are frequently applied to obtain information from a certain event, this is if enough information about the event is available and the probabilities of the event can be calculated. From an engineering point of view the bow-tie model (Figure 3) appears to be a convenient approach, combining both the fault (FTA) and event tree (ETA) to analyze a critical event. This technique provides information in terms of probabilities and/or frequencies of the possible hazards that may lead the system to fail (FTA) leading to a critical event and the consequences of this event (ETA). This information is then applied to generate preventive measures for the possible hazards and mitigation measures if the hazards cannot be avoided.

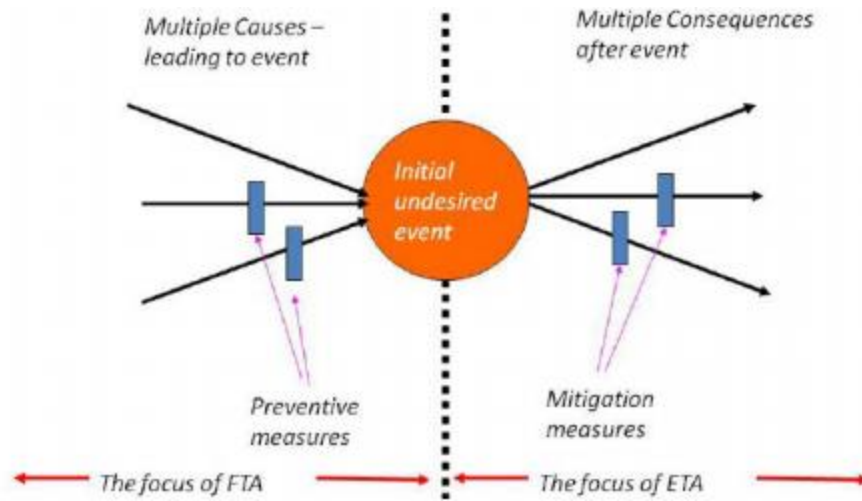


Figure 3: Concept of bow-tie model. From [8]

#### 2.3.4. Likelihood and consequences:

Estimating how likely certain events are is often perceived as one of the more difficult task in a risk assessment. Nevertheless, is one is the most important ones simply because if it is left out the risk assessment cannot be called risk assessment anymore since uncertainty is such an important part of the concept of risk. However, one should not make the mistake to associate likelihood estimation with the estimation of probabilities [7]. Estimating likelihood can be approached in a qualitative or quantitative method:

#### 2.3.5. Qualitative risk assessment:

Qualitative risk assessment methods describes the phenomena and the outcomes by establishing a ranking scale and comparing the scenarios against each other. A common type of scale for this is a five step-scale, e.g. the likelihood is expressed using a number between 1 and 5, where 1 represents the least likely and 5 the most likely. Often each of the steps on the scale is associated with a short description, such as "Likely", "Unlikely", "Very likely", etc. [7]. As for the consequences according to the severity words as "Minimal", "Minor", "Major", "Serious", "Catastrophic". The problem here is that expert judgement is relative and can differ from "expert to expert" regarding the same matter. There is no clear distinction on how likelihoods and consequences for a given scenario are considered, i.e. what would be the base in order to consider a scenario likely and the next unlikely? Personal judgment? This method is commonly applied in preliminary stages to have an idea of the possible outcomes.

### **2.3.6. Semi-quantitative risk assessment:**

Semi-quantitative risk methods simplifies the risk assessment process by introducing a ranking method to describe the level of safety or risk for a particular scenario. Expert judgement and statistical data are in charge of defining the factors affecting the levels of risk in a positive or negative aspect and providing a value for these factors and then organizing them by level of importance, e.g. extremely unlikely (less than once every 10,000 years), very unlikely (once every 1,000 years), unlikely (once every 100 years), likely (once every 10 years), very likely (more than once a year) [7]. An advantage of fire ranking methods is their simplicity considered as very cost-effective tools. Another advantage of this method is the structured way in which the decision making is treated. This facilitates understanding of the system for persons not involved in the development process and makes it easier to implement new knowledge and technology into the system [9].

## **2.4. Quantitative risk assessment**

Quantitative risk assessment method is the most complete, informative and detailed approach. It defines risk with a numerical value that can be obtained by mathematical equations and explicit assumptions relying on frequencies or probabilities to obtain results. The benefits of QRA are specified by [10] as follows:

- Considers thousands of scenarios that involve multiple failures, thus providing an in-depth understanding of system failures modes.
- Increases the probability that complex interactions between events/system/operators will be identified.
- Provides a common understanding of the problem, thus facilitating communication among various stakeholders groups.
- Is an integrated approach, thus identifying the needs for contributions from diverse disciplines.
- Focuses on uncertainty quantifications and creates a better picture of what the community of experts knows or does not know about a particular issue, providing valuable input to decisions regarding needed research in diverse disciplines.
- Facilitates risk management by identifying the dominant accidents scenarios so that resources are not wasted on items that are insignificant contributors to risk.

Among the limitations that can be mentioned are [10]:

- Human error during accident conditions. In theory human reactions are unpredictable, but experience has shown that most of the times crews often come with improvised and effective ways of mitigation when an accident occur. These human actions can't be modeled in QRA's.
- Digital software failures. The aim is not to quantify the failure probabilities but, rather, to understand the kinds of failure modes that may be introduced.

- Safety culture. While it is relatively easy to ascribe an accident to a bad safety culture, the fact is that defining indicators of good or bad safety culture in a predictive way remains elusive.
- Design and manufacturing errors. These are especially important for equipment that would require to operate under unusual conditions.

Two main points can be identified by the way experts view and analyze hazards in the risk context:

#### **2.4.1. Frequentistic or deterministic point of view**

Deterministic point of view defines the probability as a result of multiple experiments that have been carried out. Hence, the probability is defined as the number of occurrences divided by the number of experiments. The exact probability can theoretically be derived if an infinite number of experiments is carried out. In practice, usually the number of occurrences is simply divided by a sufficient number of experiments. From a deterministic point of view, the probability of tails from 1,000 coin flips with 563 times tails is 0.563 [11]. The end result are a set of curves that have to be analyzed as a whole to be able to correctly describe the meaning of risk. The input information for resolving these situations has to be tangible and clear in a way that anyone with enough information and similar background must arrive at the same end result so a definition can be described for risk regardless who is analyzing the case. The drawback of this type of method is the difficulty presented at the time to determine the input parameters that expect to produce this worst case scenario, relying on literature that may not completely apply for the specific scenario to be evaluated and the possibility of ignoring an important input and decreasing its outcome as a consequence.

#### **2.4.2. The subjective or Bayesian point of view**

Bayesian definition, on the other hand, accounts for information about a system and defines the probability as a degree of belief that an event happens and is therefore subjective. For the example of the coin flips above, it is assumed that the coin is unbiased and it is known that only heads or tails are possible results [11]. Since everyone has a different perception or interest of the task at hand, each can arrive to different conclusions of the same topic. For that reason a single outcome cannot be measured or presented in a way that reaches the same conclusion regardless of the amount of information or background of who is analyzing the case. The result would be a set of possible scenarios for a given risk and the consequences that may be produced from these risk scenarios.

The Bayesian point of view provides the most flexibility because it makes risk analysis applicable to a much broader spectrum of situations since risk analyses are often performed on systems where we don't have much statistical data. Using the Bayesian interpretation does not mean that one disregards from the information created using the frequentist interpretation and its interpretation "forces" a person to revise his/her estimation of a probability according to a

specific procedure when new information concerning the probability is revealed [12]. The method of probability distribution practiced this thesis is explained in detail in section 2.10.2.

## 2.5. Risk presentation and risk evaluation

Risk presentation is a way of compiling the information from the risk analysis into a more suitable form for decision making [7]. Risk evaluation determines if any risk is worth taking by an assessment of the profit and losses of any project analyzing the monetary losses in terms of life safety and property damages of a certain fire risk and the cost that would mean safeguard those assets and arriving to an acceptable or low as possible risk. To be able to evaluate risk this has to be presented in an easy and understandable way. 2 risk presentation methods are given below.

### 2.5.1. Risk matrix

Risk matrices maps risk levels by assigning values to the severity of the outcomes and frequency or likelihoods of occurrence for a certain scenario by a grid structure. Presenting the risk in such a way makes it easy to understand and it also provides a good overview of the system.

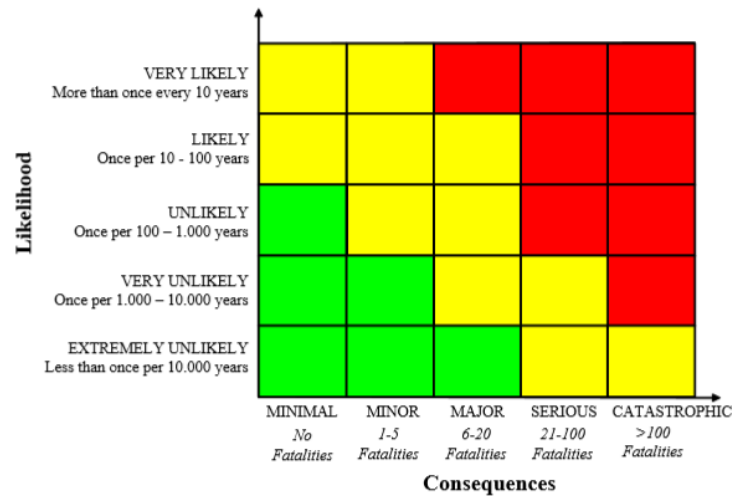


Figure 4: Risk matrix. From [7]

There are some issues that may arrive when producing a risk matrix and should be taken into account, which can be errors leading to the assignment of higher qualitative ratings to small quantitative risks and poor resolution assigning the same risk rating to very different types of risk.

### 2.5.2. FN – curves

FN – curves presents information of the consequence/frequency data about the societal risk. A number of events are taken into consideration and each will produce a predicted frequency of occurrence  $f$  in years, and a predicted number of fatalities  $N$ . The cumulative frequency of the occurrence and the number of fatalities are presented in each axis of the plot. The slope of the plot is then compared against acceptable criteria according to the jurisdiction applicable.

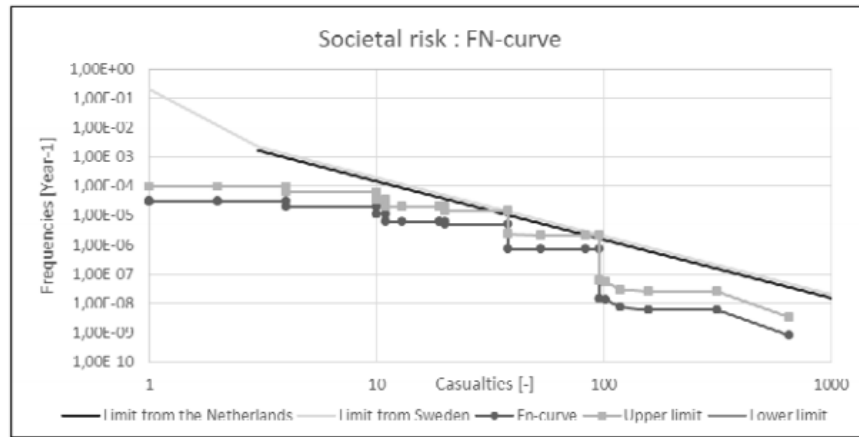


Figure 5: FN – curve for societal risk. From [8]

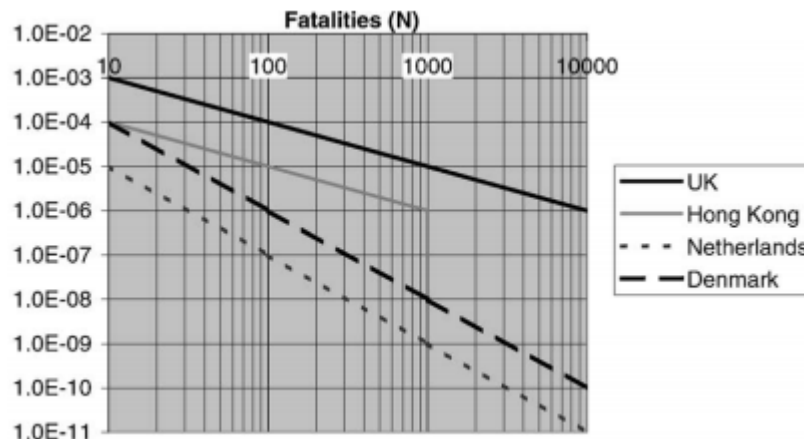


Figure 6: Comparison of international standards in FN format. From [13]

The fact that similar installation are generated in a small region should be taken into account for individual risk industries may comply with the regulation but if all those in the region are taken into account may lead to an unacceptable high risk level in a regional scale. A suggestion is made to distribute acceptable risk over regions within the nations, not over the whole nation.



## 2.6. Fire risk assessment

Fire risk assessment is a well-defined procedure for estimation of fire risk for a built environment and evaluation of estimated fire risk in terms of well-defined acceptance criteria [14]. Fire risk assessment is the most complete technique that can be applied for any fire safety analysis, taking into consideration, if desired, an infinite number of fire scenarios that can be generated by flammable products, building designs, environmental conditions or any type of potential fire risk.

It estimates the potential losses in terms of life and property damages, and offers precautions or mitigation strategies as a way to reduce as much as possible the consequences and whether these strategies are justified by a cost-benefit analysis. Fire risk assessment is not an easy task since it is not based on hard sciences like mathematics or physics but on large quantities of data from many sources, statistics and engineering judgement providing a better perspective of the problem at hand and facilitating a risk informed decision. Uncertainty in the analysis will always be present since some assumptions must be made to obtain a result, the job of the engineers is to reduce this uncertainty as much as possible.

The procedure of fire risk assessment follows the same structure and components as the general framework of risk assessment presented in figure 2 and explained in the previous sections.

Fire safety engineering has relied on prescriptive methods to determine its designs which are based on a set of regulations and delimitations that every building must comply in order to be deemed acceptable in terms of fire safety, i.e. maximum allowable distances to exits, specific structural materials of the building... this facilitates its application but it does not necessarily mean that is the best choice to follow. Its inflexibility regarding the safety measures and the fact that it is very general may result in unnecessarily implementation of systems for particular enclosures with unique designs.

Performance based design is defined by [1] as an engineering approach to fire protection design based on (1) agreed upon fire safety goals and objectives, (2) deterministic and/or probabilistic analysis of fire scenarios, and (3) quantitative assessment of design alternatives against the fire safety goals and objectives using accepted engineering tools, methodologies and performance criteria. The four fundamental for fire safety are: life safety, property protection, mission continuity and environmental protection.

Designs that comply with the prescriptive option of NFPA 101 or NFPA 5000 are “deemed” to comply with the goals specified by the codes. However, designers who prepare performance-based designs would have to demonstrate that they achieve the goals of the applicable code [15]. PBD allows the designer to address unique features present for each individual case and allows a better understanding of the building in case of fire. The setback of PBD is that it requires a deeper understanding of the fire phenomena and more time, in comparison with a prescriptive design, for the elaboration.

## 2.7. Life safety criteria

Life safety criteria addresses the survivability of people exposed to fire or fire products. The values selected as performance criteria might vary depending on the physical and mental conditions of building occupants and length of exposure. Performance criteria may need to be developed in the areas of the thermal effects to people (e.g., exposure to high gas temperatures or thermal radiation), toxicity of fire products, or visibility through smoke [15]. The performance of the building in case of fire is considered acceptable if the available safe egress time (ASET) for the people to evacuate is larger than the required safe egress time (RSET) due to the fire conditions.

$$\text{ASET} > \text{RSET} \quad (2)$$

Required safe egress time (RSET) would then be defined as the sum of: the ignition to the detection time + the time of the detection to the notification of occupants + the time until the occupants start to take action + the time when the evacuation starts + the time when the evacuation is finished.

ASET is defined as the time in which the fire enclosure reaches critical conditions. The ASET value varies according to different building configurations, construction materials, fuel packages, ventilation conditions. The main hazards for people in a fire-induced environment are [15]:

### 2.7.1. Thermal injuries.

Thermal injuries can be caused by immersion of an individual in a heated atmosphere or by radiant transfer. In general, as long as an individual is exposed to thermal radiation below a threshold of around  $1 \text{ kW/m}^2$  the person will not experience pain or burns, even for long exposures [15]. The occupants of an enclosure can be assumed to be safe from any thermal injuries or hyperthermia, considered as the primary hazard, as long as the room temperature remains below  $80 \text{ }^\circ\text{C}$ .

### 2.7.2. Toxicity.

Toxicity is defined as the degree which a harmful substance can have a negative physiological or pathological effect over an organism. In the case of fire physiological effects are of most importance determining whether or not a person is able to evacuate a location in case of fire. The level which toxic gas has an effect over an organism depends on the following factors:

- The time of exposure.
- The concentration of toxic gasses during exposure, i.e. toxic gasses will have a higher concentration in the ambient the longer the fire burns or pyrolyse.
- The toxic potency of the gasses.

Toxic product yields depend on the fire conditions and the type of burning material. The effects from toxic gasses alternates from person to person according to their constitution, age and health. The consequences may vary from thermal effects to irritation of respiratory system and central nervous system depression. Lethality and incapacitation concentrations can be computed by the fractional effective concentration or FED and by the fractional incapacitation concentration or FEC.

$$FED = \frac{\text{Concentration of gas present} \times \text{time}}{\text{Specific dose to produce lethality}} \quad (3)$$

$$FEC = \frac{\text{Concentration of gas present}}{\text{Concentration causing irritant effect}} \quad (4)$$

FED or FEC values of 1.0 are associated with sublethal effects that would incapacitate people of average susceptibility [16]. The most common toxic gases produced in case of fire are CO<sub>2</sub>, CO and HCN.

### 2.7.3. Reduction of visibility.

Visibility itself does not cause any physiological harm but it limits the capacity of the occupants of finding escape routes. Reduce visibility can impact human behavior in many ways [15]:

- Reduce the likelihood that people will move through an egress route.
- Reduce movement speed of egress route.
- Reduce way finding ability.

Figure 7 shows the impact of irritant and not irritant gasses on walking speeds. Besides the reduction of walking speed the loss of visibility decreases the ability of finding the egress routes, making this task especially difficult for those occupants not familiarized with the building surroundings, where  $C_s$  denotes the extinction coefficient in smoke that can be related to visibility in smoke and studies has shown that once the extinction coefficient surpasses a threshold of  $0.55 \text{ m}^{-1}$  for irritant gases the visibility drops so zero.  $C_s$  can also be related to obscuration units in smoke.

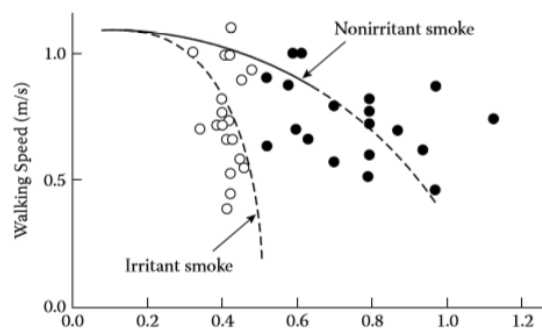


Figure 7: Walking speed in fire smoke. From [1]

Table 1 sums up the critical conditions in a fire enclosure that determines the ASET.

<b>Parameter</b>	<b>Value</b>
Radiation (dose)	60 kJ/m <sup>2</sup>
Radiation (10 minutes)	2.5 kW/m <sup>2</sup>
Radiation (long)	1 kW/m <sup>2</sup>
Smoke layer height	1.6 + (0.1h) m
Visibility	10 m / 5 m
Temperature	80 °C

**Table 1: Critical conditions in fire enclosures. From [1]**

## 2.8. Fire Computer Models

### 2.8.1. Definition of fire computer models.

Computer programs design to simulate a process, involving a representation of a fire (typically within an enclosure) and the effects over property and people. Even though manual calculations are acceptable for a fire protection design, these are not well suited when they have time dependent interactions. What these programs do is to facilitate the work by performing a large amount of calculations in a fraction of the time required for manual work and present an accurate representation of reality.

Fire models can be divided into: zone models and CFD models.

### 2.8.2. Zone models.

Zone models solve the conservation of mass and conservation of energy equations. Its basics assumptions are:

- The room is divided into two zones: hot upper layer and the cold bottom layer.
- The conditions inside each layer are uniform.
- There is horizontal plane between layers called ‘interface layer’.
- The position of the ‘interface layer’ can vary over time.
- The conditions of within the layers can vary over time.

Zone models are used in preliminary stages of the design providing a first order estimate of the fire. In conclusion zone models are programmed versions of simplified calculations that are well suited for small compartments and comparative studies, in reality there is no clear distinction between layers as it is in zone models.

The most common fire zone models are listed in table 2.

Model Name	Author(s)	Maintaining Organization	Special Features
Branzfire	C. Wade	Building research institute of New Zealand Incorporated	Multiroom, corner fires, mechanical ventilation
Ozone	J.F. Cadorin, D. Pintea, J.C. Dotreppe, J.M. Franssen	E.C.C.S., University of Liege, Arcelor Research	Multitoom, gas temperatures, steel temperatures
ASET	L. Y. Cooper, D. W. Stroup	NIST	Single room
ASET-B	W. D. Walton	NIST	Single room

BRI2	K. Harada, D. Nii, T. Tanaka, S. Yamada	Building Research Institute, Japan	Multiroom, mechanical ventilation
CCFM-VENTS	L. Y. Cooper, G. P. Forney	NIST	Multiroom, multilevel
COMPBRN III	N. Siu, V. Ho	UCLA	Single room, developed for nuclear power facilities
COMPF2	V. Brabuskas	NIST	Single room, postflashover
FAST/CFAST	R. D. Peacock, P. A. Reneke, W. W. Jones, R. W. Bukowski, G. P. Forney,	NIST	Up to 30 compartments, 30 ducts and 5 fans
FIRST	H. W. Emmons, H. E. Mitler	NIST	Single room, burning item
WPI/FIRE	D. B. Satterfield, J. R. Barnett	WPI	Single room, ceiling vents

**Table 2. Enclosure zone fire models. Adapted from [17]**

The zone model employed in this thesis is CFAST, a brief description of its functions is given below [17].

FAST/CFAST (Consolidated Model of Fire Growth and Smoke Transport): is a multiroom fire model that predicts the conditions resulting from a user-specified fire within a structure. The required program inputs are the geometrical data describing the rooms and connections: the thermophysical properties of the ceiling, walls and floors; the fire as a rate of mass loss; and the generation rates of the products of combustion. The program outputs are the temperature and thickness of, and species concentrations in, the hot upper layer and the cooler lower layer of each compartment. Also given surface temperature, heat transfer, and mass flow rates. The distribution software includes graphic and text report generators, a plotting package, and a system for comparing results from multiple simulations.

### 2.8.3. CFD.

Computational fluid dynamics are the most sophisticated fire models solving the fundamental equations of mass, momentum and energy by modelling and using numerical methods discretizing in time and space (Navier-Stokes equations) to obtain results. There are different solutions methods which if applied correctly does not affect the result and these are:

- Finite elements.
- Finite volumes.
- Finite differences.

The idea is that the enclosure is divided into grids (tiny imaginary cubes) known as meshes and the finer they are the more accurate results, but this also produces a problem which is time steps must be smaller for smaller control volumes. In consequence much more computer time and memory is needed to resolve the finer meshes. The CFD model calculates the physical conditions in each cube and the changes over time by an iterative solver allowing the user to check the conditions at any time and place of the enclosure.

The CFD process for any model is the same and can be divided into:

- Pre-processor: the construction of the geometry and the computational mesh is executed, the physical and chemical models are chosen, the boundary conditions, the fluid and solid properties are defined and the time step desired is defined.
- Solver: Once the input information from the pre-processor is defined, the unknowns are computed and the algebraic equations are solved
- Post-processor: all the output and input information is visualized.

There are different sub-models for turbulence, combustion, radiation... and these are usually predetermined by the models, some models allow the options to change the sub-model to the one desired for the execution of the program such as RANS or LES for turbulence.

The most common CFD models are listed in table 3.

<b>Model Name</b>	<b>Author(s)</b>	<b>Maintaining Organization</b>	<b>Applications and Special Features</b>
ALOFT-FT	W. D. Walton, K. B. McGratten	NIST (U.S.)	Smoke plumes from outdoor fires
CFX-4	AEA Technology	AEA Technology	General purpose computational fluid dynamics (CFD) codes

FDS	K. McGratten, H. Baum, R. Rehm, A. Hamins, G. Forney	NIST (U.S.)	3-D Large Eddy Simulation (LES) model for fires in multicompartments with sprinkler suppression capabilities
FISCO-3L	V. Scheider, J. Hoffmann	INTELLEX, FR (Germany)	Single room treatment for fire development
JASMINE	G. Cox, S. Kumar	Sintef (Norway)	Analysis of smoke movement
KAMELEON FIRE E-3D	B. F. Magnussen	Fire Research Station (U.K.)	Single room fire growth model for pool fires
KAMELEON II	B. F. Magnussen	NTH/SINTEF (Norway)	Multiroom fire and smoke spread
KOBRA-3D	INTELLEX	INTELLEX (Germany)	3-D CFD model for determining hydrodynamical flow in a single fire compartment
PHOENICS	D. B. Spalding	CHAM, Ltd. (U.K.)	A general purpose 3-D transient fluid dynamics code
RMFIRE	G. Hadjisophocleous	National Research Council of Canada (Canada)	A 2-D CFD model for transient calculations of smoke movement in a room fire
SPLASH	A. J. Gardiner	South Bank Polytechnic (U.K.)	A quasi-CFD model describing the interactions of sprinkler sprays with fire gases
STAR*CD	D. Gossman, R. Issa	Computational Dynamics (U.K.)	General-purpose computational fluid dynamics (CFD) code

Table 3. CFD fire models. Adapted from [17]

The CFD model employed in this thesis is FDS 6, a brief description of its functions is given below [17].

FDS: The Fire Dynamics Simulator (FDS) allows for “Direct Numerical Simulation” or “Large Eddy Simulation (LES)” of fire. The LES approach most readily lends itself to solving the types of fire problems typically found in fire engineering design and forensic applications. LES uses a low Mach number approximation for the Navier-Stokes equations. Under the Les mode, the user inputs the parameters of the fire in terms of heat release rate and species generation. The fire is modeled



as Lagrangian particles that release heat. FDS calculates the temperature, pressure, species concentrations and flow field in relation to the prescribed fire. FDS provides for calculating the activation of heat detectors and sprinklers. In addition the sprinklers can dispense droplets, which yield evaporative cooling and prewetting. The model supports predictions of multiple sprinkler activations. The geometry is rectilinear with description of the overall computational domain. Within the computational domain, sections can be delineated as walls or vents. The model also supports heat-activated vents that “open” allowing flow through the vent. Smokeview is the companion software designed to visualize the numerical predictions generated by FDS.

## **2.9. Sensitivity analysis**

### **2.9.1. Definition of sensitivity analysis**

Sensitivity analysis, as it is applied to risk assessment, is any systematic common sense technique used to understand how risk estimates and, in particular, risk-based decisions, are dependent on variability and uncertainty in the factors contributing to risk. In short, sensitivity analysis identifies what is “driving” the risk estimates. It is used in both point estimate and probabilistic approaches to identify and rank important sources of variability as well as important sources of uncertainty [18].

A preceding sensitivity analysis allows us to reduce the number of random variables that are present in any particular case. There are many sensitivity analysis models some more complex than others and each with their own strengths and weaknesses. How to decide one comes down to the following factors [19]:

- The computational cost of running the model.
- The number of input factors.
- The degree of complexity of the model coding.
- The amount of analyst’s time involved in the sensitivity analysis.
- The setting of the analysis.

Sensitivity analysis can be categorized into [20]:

- Local sensitivity measures, are based on estimation of partial derivatives, and assess how uncertainty in one factor affects the model output keeping the other factors fixed at a nominal value. The main drawback of this approach is that interactions among factors cannot be detected, since they become evident when inputs are changed simultaneously.
- Global measures offer instead a comprehensive approach to model analysis, since they evaluate the effect of a factor while all others are varying as well, exploring efficiently the multidimensional space.

## **2.10. Sensitivity Analysis methods**

### **2.10.1. Morris method**

The Morris method is a randomized one factor at a time design, and data analysis based on the resulting random sample of observed elementary effects, those changes in an output due solely to changes in a particular input [21]. It introduced the elementary effect method as a way of determining the most influential parameters of the region of interest.

– Trajectories

The region of experimentation  $\Omega$  is a  $k$ -dimensional unit cube (standardized) over which the input vector  $x$  is uniformly distributed [22]. The computation of each elementary effect requires two sample points, the simplest design would require  $2r$  sample points for each input, for a total of  $2rk$ , where  $k$  is the number of input factors while  $r$  is the number of points. Morris suggested a more efficient design that builds  $r$  trajectories of  $(k+1)$  points for the input space, each providing  $k$  elementary effects, one per input, for a total sample points of [23]:

$$r(k+1) \quad (5)$$

The trajectories are generated in the following manner. A base value called  $x^{(1)}$  located in the  $p$ -level grid  $\Omega$  is selected,  $x^{(1)}$  is not part of the trajectories itself but it's the reference point for the first trajectory. To generate the first trajectory, one and only one of the  $k$  components  $x^*$  is raised by a value  $\Delta$ , where  $\Delta$  is a predetermined multiple of  $1/(p-1)$  and  $p$  is the number of levels chosen for the calculations producing a new point  $x^{(2)}$ , i.e.  $x^{(2)} = x^{(1)} + \Delta$ . The value  $x^{(2)}$  is now the new base point for trajectory 2, produced in the same manner by raising or decreasing a value of  $\Delta$  of one  $k$  components of  $x^{(*)}$  resulting in a new point  $x^{(3)}$ , i.e.  $x^{(3)} = x^{(2)} + \Delta$  and it goes on until  $x_{k+1}$ . Every value  $x$  generated will always be inside  $\Omega$ .

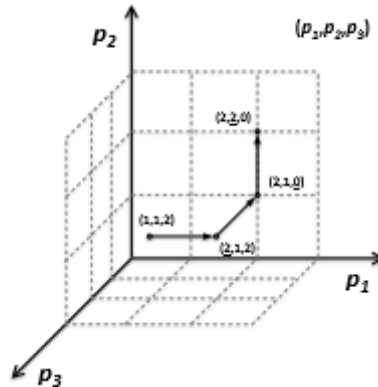


Figure 8: Example of a trajectory in the input space when  $k=3$ , using points  $(1,1,2)$  as base points. From [27]

– Sampling strategy

The technical scheme to generate the sampling trajectories can be seen in the form of a matrix,  $B^*$ , with dimensions  $(k+1) \times k$ , whose rows are the vectors  $x^{(1)}, x^{(2)}, \dots, x^{(k+1)}$ . The first step is to build the matrix  $B$  with same dimensions and holds 0's and 1's and the property that for every column index  $j, j = 1, \dots, k$ , there are two rows of  $B$  that differ only in the  $j$ th entry. A convenient choice for  $B$  is a strictly lower triangle matrix of 1s [23].

$$B = \begin{bmatrix} 0 & 0 & 0 & \dots & 0 \\ 1 & 0 & 0 & \dots & 0 \\ 1 & 1 & 0 & \dots & 0 \\ 1 & 1 & 1 & 0 & \dots \\ \dots & \dots & \dots & \dots & \dots \end{bmatrix}$$

The matrix  $B'$ , given by

$$B' = J_{k+1,k} x^* + \Delta B \quad (6)$$

Where  $J_{k+1,1}$  is a  $(k+1) \times k$  matrix of 1's and  $x^*$  is a randomly chosen base value of  $x$ , is a potential candidate for the desired matrix, but it has the limitation that the  $k^{\text{th}}$  Elementary effect is produced would not be randomly selected. A randomized version of the sampling matrix is given by [23]:

$$B^* = (J_{k+1,1} x^* + (\Delta/2)[(2B - J_{k+1,k})D^* + J_{k+1,k}]) P^* \quad (7)$$

Where  $D^*$  is a  $k$ -dimensional diagonal matrix in which each element either +1 or -1 with equal probability, and  $P^*$  is a  $k$  by  $k$  matrix random permutation matrix [19].

An enhancement of the sampling trajectories is introduced on the basis that the design of generating random sampling points for each trajectory may not be the best option to cover the input space of interest. The idea is to select  $r$  trajectories in such a way to maximize their dispersion over the input space. The first step is to generate a large number of trajectories and then selecting a value of  $r$  with the highest spread. The concept of spread is defined by distance, this distance is equal to the distance between two trajectories  $m$  and  $l$  and is defined by equation 8 [24].

$$d_{ml} = \begin{cases} \sum_{i=1}^{k+1} \sum_{j=1}^{k+1} \sqrt{\sum_{z=1}^k [X_i^{(m)}(z) - X_z^{(l)}(z)]^2} & m \neq l \\ 0 & \text{Otherwise} \end{cases} \quad (8)$$

Where  $k$  is the number of input factors and  $X_i^{(m)}(z)$  indicates the  $z$ th coordinate of the  $i$ th point of the  $m$ th Morris trajectory [25]. Figures 9 and 10 shows a comparison between both methods of generating trajectories.

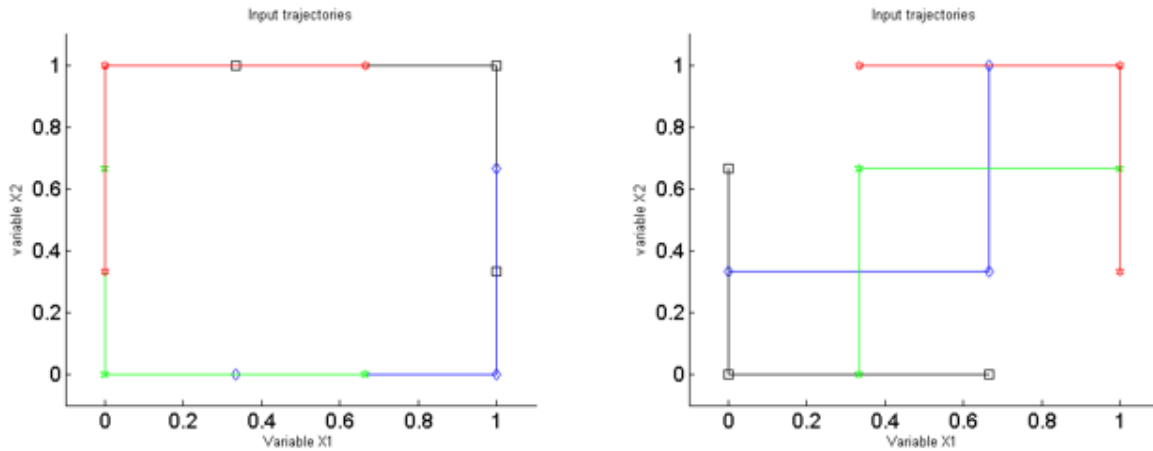


Figure 9: Optimized trajectory with all possible combinations (left) trajectories pushed to the outside (right) optimized trajectories with second criterion ( $p=4, r=4$  &  $m=6$ ). From [22]

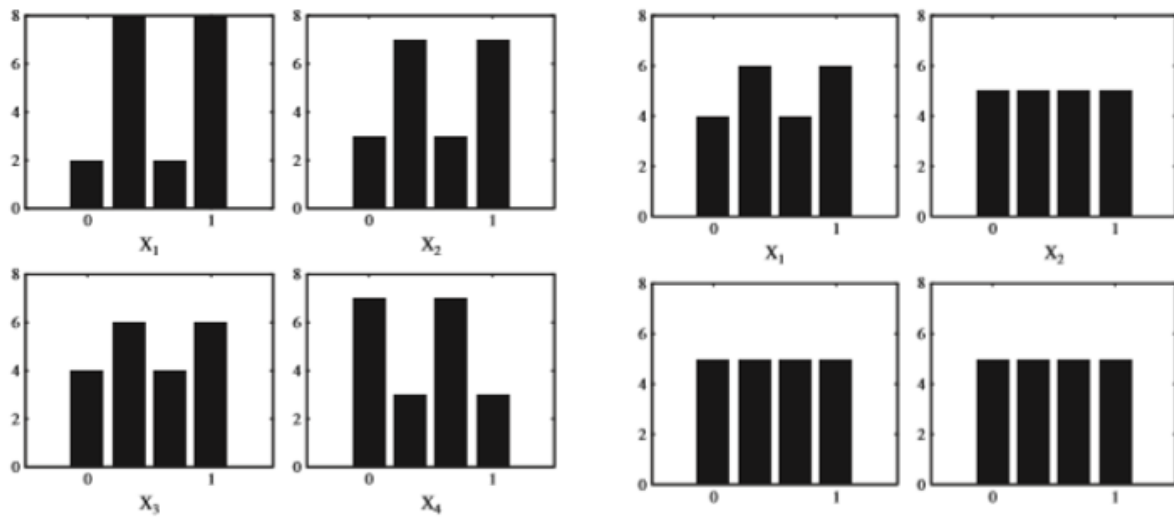


Figure 10: Original sampling strategy (left) and improved strategy (right). From [24]

Where  $x_1, x_2, x_3$  and  $x_4$  are sample values whose theoretical distributions are uniform discrete with 4 levels. The original  $r = 20$ .

– Elementary effect Method

The guiding philosophy of the EE method is to determine, within reasonable uncertainty, which input parameters may be considered to have effects which are (a) negligible, (b) linear and additive, (c) nonlinear, (c) involved with interactions with other inputs [24].

The EE is denoted as:

$$d_i(\mathbf{x}) = \frac{[y(x_1, x_2, \dots, x_{i-1}, x_i + \Delta, x_{i+1}, \dots, x_k) - y(x)]}{\Delta} \quad (9)$$

The mean and standard deviation for each variable are used to determine whether a factor has any effect in an output and if it has a significant interactions with other factors.

$$\mu_i = \frac{1}{r} \sum_{j=1}^r EE_i^j \quad (10)$$

$$\sigma^2 = \frac{1}{r-1} \sum_{j=1}^r (EE_i^j - \mu)^2 \quad (11)$$

A high  $\mu$  represent that the input factor has a high influence in the output while a high  $\sigma$  represents that the factor has high interaction with other factors or a not linear behavior. The distribution of elementary effects associated with the  $i$ th input factor is obtained by randomly sampling different  $x$  from  $\Omega$ , and is denoted by  $F_i$ , i.e.  $EE_i \sim F_i$  [25].

An improvement to this method was proposed to prevent cancellation of products with different sign and in consequence it may fail to consider important factors. To do so it was proposed a refinement of  $\mu$  to a now named  $\mu^*$  which is the estimate of the mean of the distribution of the absolute values of the elementary effect [25]. The result is:

$$\mu_i^* = \frac{1}{r} \sum_{j=1}^r |EE_i^j| \quad (12)$$

The distribution of the absolute values of the elementary effects that we denote with  $G_i$ , i.e.  $|EE_i| \sim G_i$  [25]. The drawback of calculating the mean with absolute values is the loss of the information on the sign of the effect. Nevertheless, this information can be recovered by the simultaneous examination of  $\mu$  and  $\mu^*$ , as an estimate of  $\mu$  comes at no extra computational cost [25].

### 2.10.2. Radial OAT experiments and Sobol sequence

An alternative design to compute the elementary effects based on a radial-like configuration [20]. The method is defined as follows. The first step is to determine a point  $x^{(1)}$  located inside  $\Omega$ , this will be the base point or reference point from which all trajectories are generated. The first trajectory is created by varying  $x^{(1)}$  in one and only one coordinate/dimension, this will be point  $x^{(2)}$ . The following trajectory is generated by going back to the base point and varying one coordinate/dimension different than the one selected by trajectory one, this will go on until reaching  $x^{(k+1)}$ .

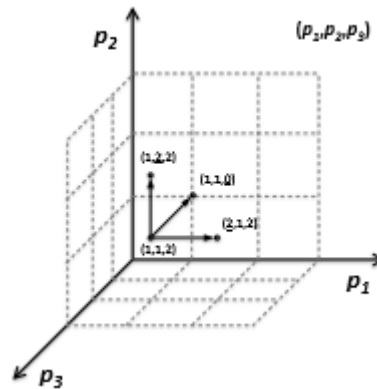


Figure 11: Example of a radial trajectory in the input space when  $k=3$ , using points  $(1,1,2)$  as base points. From [27]

The elementary effect method is calculated in a different manner than the one proposed by Morris (1991), the step size for this case is different being now the distance between two points denoted by a sampling matrix e.g.  $x_i^{(u)} x_{\sim i}^{(u)}$  and  $x_i^{(v)} x_{\sim i}^{(v)}$  which is to say the difference between  $x_i^{(u)}$  and  $x_i^{(v)}$ , where  $u$  and  $v$  denote two rows of the sampling matrix. The elementary effect will then be:

$$EE_i = \frac{y(x_i^{(u)} x_{\sim i}^{(u)}) - y(x_i^{(v)} x_{\sim i}^{(v)})}{x_i^{(u)} - x_i^{(v)}} \quad (13)$$

The methods for computing  $\mu$ ,  $\mu^*$  and  $\sigma$  remains as described in equations 10, 11 and 12

#### – Sobol quasi-random sequence

Sobol quasi-random sequence is used to generate and uniformly distribute a set of numbers over the unit hypercube  $\Omega$ , quasi-random numbers know about the position of previously random points and fill the gaps between them. [26]. A Sobol sequence is produced and can be used to identify points inside the  $\Omega$  hypercube. Each point of a Sobol sequence consist in a numerical value between one and zero. A collection of these values may be used to identify a specific point

in a parameter space. An element of a point of a Sobol sequence can be converted into a parameter value by some normalization process [27].

0.95	0.75	0.5	0.5	0.5
0.9375	0.75	0.5	0.5	0.5
0.95	0.8125	0.5	0.5	0.5
0.95	0.75	0.125	0.5	0.5
0.95	0.75	0.5	0.625	0.5
0.95	0.75	0.5	0.5	0.375

Table 4: five-dimensional Sobol quasi-random sequence, first five points. Normalized values [0,1]

An example on how to compute the elementary effect output is shown in table 5. The probabilistic values are obtained by a Sobol sequence and radial trajectories.

Point	Probabilities of QR numbers	Normalized values of $\alpha$ (kW/s <sup>2</sup> )	$x_i^{(u,v)} x_{\sim i}^{(u,v)}$
base	0.965	0.05072573	20.146877
auxiliary	0.95625	0.03975837	20.170704

Table 5: Sobol quasi-random sequence and radial trajectories

Calculating EE:

$$EE_i = \frac{20.170704 - 20.146877}{0.965 - 0.95625}$$

A good practice when generating a Sobol quasi-random sequence is [26]:

1. The uniformity of the quasi-random sequence is linked to the ordered and progressive filling of space, which is filled at a given density, every  $2^m$  points ( $m=1, 2, \dots$ ). Thus, it would be a mistake to skip rows of the quasi-random matrix.
2. The uniformity of the quasi-random matrix deteriorates as the column index increases, i.e. the first column of the matrix would be the best equally distributed following would be the second and so on.



– Total Sensitivity Index

Via the screening experiment the modeler gets a first insight of the model behavior and can for instance understand if a revision is needed, due for instance that some factors intended as important are actually not influencing the model response. In alternative, using the proposed design, if the computational cost of the model allows it, the modeler can increase  $r$ , the number of repetitions, up to achieve a sample size compatible with the estimation of the total sensitivity index STi (Equation 14) [20]. Which is basically the sum of each individual effect.

$$S_{Ti} = \frac{V_{Ti}(Y)}{V(Y)} = \frac{E_{X \sim i}(V_{Xi}(Y|X \sim i))}{V(Y)} \quad (14)$$

And

$$E_{X \sim i}(V_{Xi}(Y|X \sim i)) = \frac{1}{2r} \sum_{j=1}^r (y(a_1^{(j)}, a_2^{(j)}, \dots, a_k^{(j)}) - y(a_1^{(j)}, a_2^{(j)}, \dots, b_i^{(j)}, \dots, a_k^{(j)}))^2 \quad (15)$$

Where  $a^{(j)}$  is the  $j$ th baseline point and  $b^{(j)}$  is the  $j$ th auxiliary point.

$V(Y)$  is the output variance determined by equation 16 that can be computed by decomposing the output variance in terms of main effect and residual [28].

$$V(Y) = V(E(Y|X \sim i)) + V(E(Y|X \sim i)) \quad (16)$$

## 3. Case Study

### 3.1. Approach

The analysis is carried out by the elementary effect method described in sections 2.10.1, 2.10.2 equations 10 to 13 and by the computation of the total sensitivity index presented in section 2.10.2 equations 14 to 16 with the objective to understand the most significant parameters in case of life safety. The parameters selected for evaluation are those related to the physical properties of the fuel packages and considered, according to expert judgement, to have a major impact on life safety in case of fire regarding the temperature of the enclosures and the toxicity levels (CO analyzed only).

5 cases are evaluated, each case with  $r ( k + 1 )$  possible scenarios with  $r = 6$  and  $k = 5$ , as defined by equation 5, resulting in a total of 180 scenarios. The models selected to carry out the CFD simulations are FDS version 6 from National Institute of Standards and Technology (NIST) and the zone model is CFAST 7.1.1. There is no particular reason for the selection of these models other than it can be downloaded for free and it gives an accurate prediction of the fire phenomena. The default turbulence, combustion and radiation models for FDS (LES, mixture fraction based and thermal radiation transport) are used for the calculations.

The parameters of interest are:

- Growth rate: During the pre-flashover phase this parameter will determine the rate at which the fire spreads over the burning area allowing the prediction of the flashover time.
- HRRPUA: Together with the burning area will determine the HRR regarded as the most important parameter in a fire.
- Area of the fuel: As previously mentioned, together with the HRRPUA will determine the HRR. The area of the fire will determine the height of the flame which has a direct influence on the radiative heat fluxes to surrounding objects and on the air entrainment and thus on the convective heating of the objects in the upper layer [29].
- Heat of combustion: It is also a factor determining the HRR of the fire, affecting the flame height as well. Decreasing the heat of combustion while keeping the HRR and the fire area fixed, results in an increase of the pyrolyzate mass flow per unit area (and vice versa) [29]
- CO yield: Determining the CO production within the enclosure, one of the primary gases in regards with toxicity.

The output parameters to be evaluated are:

- Temperature.
- CO levels.

The procedure and evaluation method is the same for every case varying only in geometry, conditions within the enclosure and location of the fire source. The procedure for the calculations is presented as follows:

1. Determine the values of the input parameters. The method described in section 2.10.2 Sobol quasi-random sequence in combination with radial sampling is applied. The statistical simulations to determine the values for the Sobol quasi-random sequence are carried out with the help of UQLab [30]. The process carried out is presented as follows:
  - Define the physical model and establish the minimum and maximum values for the parameters of interest.
  - Estimate the distribution of the parameters.
  - Execute the calculations.
  
2. 5 different case scenarios are evaluated each with 6 trajectories (5 variables + 1) and 6 different base points per scenario. The values obtained by the matrix generated in step 1 will serve as input parameters for the CFD and zone model calculations.

Tables 6 and 7 show the ranges of values from which the input parameters will be varying and the average and standard deviation employed.

	A	HRRPUA	Max area	HOC	CO-yield
	kW/s <sup>2</sup>	kW/m <sup>2</sup>	m <sup>2</sup>	kJ/kg	g/g
Min	0.024714	289.4648	2.492537	18863.52	0.028635
Max	0.132207	531.4849	51.76137	29601.4	0.151365

**Table 6: Range of values of input parameters**

Parameter	Type	$\mu$ log	$\sigma$ log
$\alpha$ -growth	Lognormal	-6.6	2.2
HRRPUA	Lognormal	0.78	1.7
Max area	Lognormal	5.971854	0.198042
HOC	Normal	25000	4000
CO-yield	Normal	0.09	0.04

**Table 7: Mean and standard deviation for input parameters**

The chosen values for  $\alpha$  would mostly fall in the denominated fast growing fire rate according to [31] the reason is that a slow growing fire may reduce the rate of toxic hazard development and increase the time available for escape or firefighting [32], the result of slow growing fires would then be no fatalities due to the fact that the available escape time would be large enough to allow every occupant to escape. Figure 12 shows the energy release rates for different growth rates and table 8 presents the values of  $\alpha$  for different growth rates according to [31].

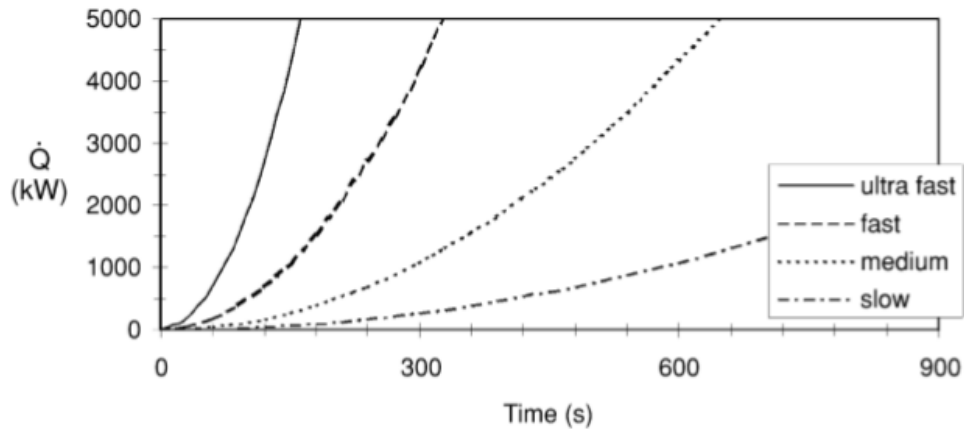


Figure 12: Energy release rates for different growth rates. From [35]

Growth rate	$\alpha$ (kW/s <sup>2</sup> )	Time (s) to reach 1055 kW
ultra-fast	0.19	75
fast	0.047	150
medium	0.12	300
slow	0.003	600

Table 8: Values of  $\alpha$  for different growth rates. Adapted from [31]

- Once all of the fire simulations are completed, results are evaluated focusing on temperature and CO levels within the enclosure at height 1.5 meters in locations defined in sections 3.2.1 and 3.2.2 for the CFD cases. For the zone model the temperature will also be measured at the same points and height as the CFD model but CFAST does not allow the possibility to measure the CO levels at an specific height, allowing only the measure of the CO levels within the upper or lower layer, given that the upper layer typically descend within 2 minutes of the fire initiation then the measurements will be taken from the upper layer.

The elementary effect method described in section 2.10.1 equations 10 to 13 is applied to calculate the standard deviation  $\sigma$  and the mean of the absolute values  $\mu^*$ . This is done for every time step of the output.

4. The total sensitivity index presented section 2.10.2 equations 14 to 16 is computed as an alternative sensitivity analysis method, determining the influence of the input parameters over the output.

## 3.2. Setup

### 3.2.1. Case 1: Retail shop

Figure 13 shows a layout of the retail shop.

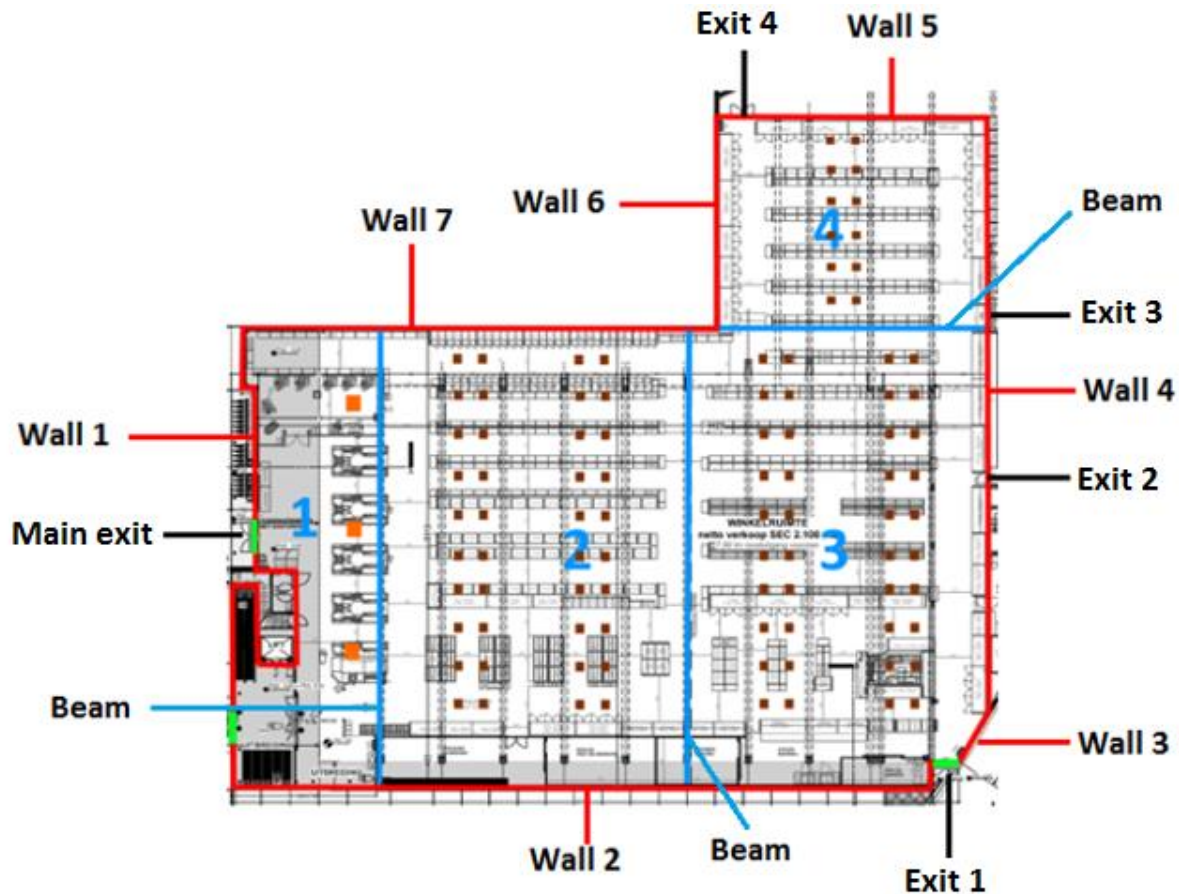


Figure 13: Retail shop layout

Wall 1 is taken as a single unobstructed wall following a straight line over the entire section like any of the other walls in figure 13, the dimensions of the exits are given in table 9. Three beams delimitate each section of the enclosure, the beams have dimensions of 0.5 m width x 0.5 m height. The obstructions presented are shop items and counters. Sections 1 and 2 have a mesh size of 0.25 x 0.25 x 0.25 m while section 3 and 4 have a mesh size of 0.50 x 0.50 x 0.50 m, the meshes are not as refined as section 1 and 2 due the large dimensions of the enclosure resulting in a high computing time to evaluate an enclosure with a such refined mesh size. The height of the ceiling is 3 m. The total area of the enclosure is 2310  $m^2$ .

Description	Length/Width (m)	Height (m)
Main exit	2.0	2.2
Exit 1	2.0	2.2
Exit 2	0.8	2.2
Exit 3	0.8	2.2
Exit 4	2.0	2.2

Table 9: Exit dimensions

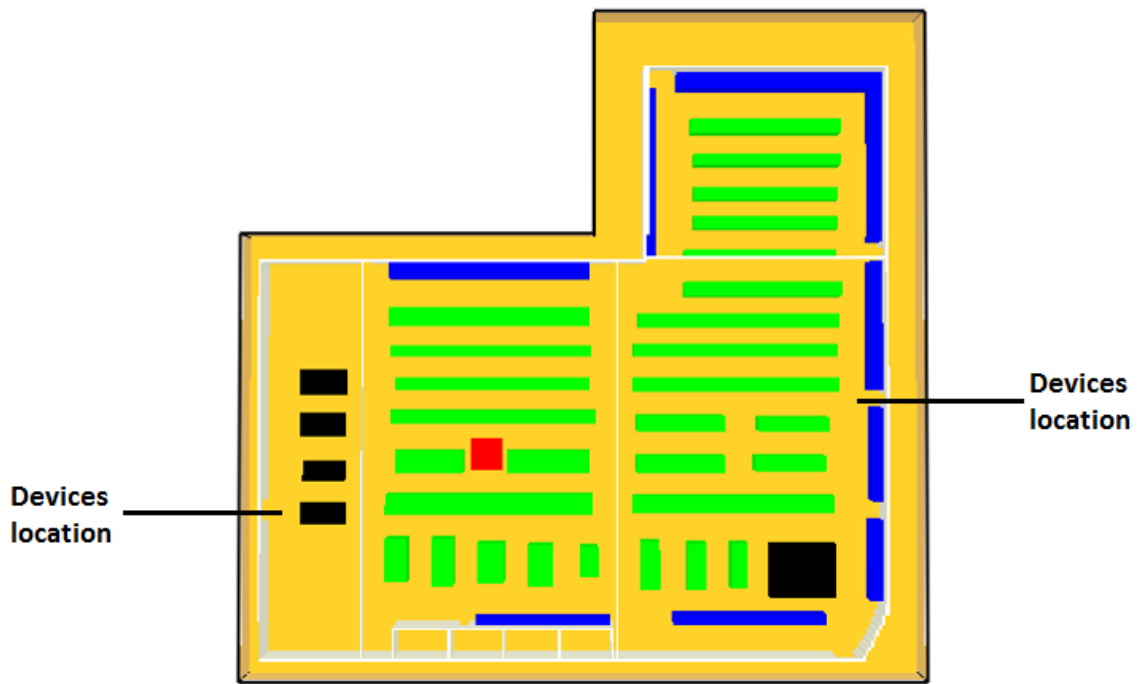


Figure 14: Retail shop FDS layout and location of devices

The location of the devices measuring outputs at the main exit and at exit 2 at 1.5 meters height as shown in figure 14.

### 3.2.2. Case 2: Bar

Figure 15 shows the FDS layout for the bar and the location of the devices.

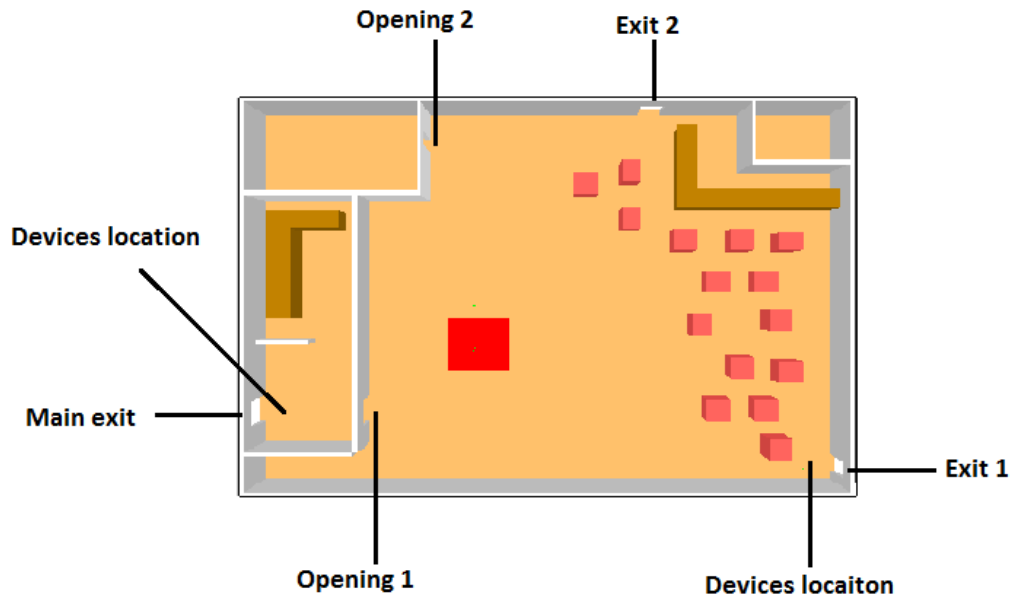


Figure 15: FDS bar layout and devices location

The dimensions of the enclosure are 20 m length x 12 m width. The devices measuring the output are located in front of the main exit and exit 1 at 1.5 meters height. The height of the ceiling is 3 m, the dimensions of the exits and openings are given in table 10. The mesh size for the entire configuration is 0.2 x 0.2 x 0.2 m. The total area of the enclosure is 240  $m^2$ .

Description	Length/Width (m)	Height (m)
Main exit	1.2	2
Exit 1 and 2	0.8	2
Opening 1 and 2	0.8	2

Table 10: Exits and opening dimensions



### 3.2.3. Case 3: Bar with sprinkler system

The layout for the third case of study is the same as described in section 3.2.2. In this case, sprinklers are added to the concept.

The activation time for sprinklers is dependent on diverse factors, i.e. the HRR of the fire, the activation temperature of the sprinkler, the ceiling jet velocities, the location of the sprinkler relevant to the fire, the height of the ceiling and the ambient temperature. It is not the purpose of this thesis to fully investigate and evaluate these factors. However, we will determine through CFD simulations the time when the temperature at sprinkler location reaches 58 °C and assume that at this point the sprinkler system is activated. This is calculated by evaluating the growth rate of the fire determining how fast is the heat released from the fire and in consequence increasing the temperature within the enclosure. Four CFD simulations are carried out evaluating four different growth rates that will represent the times for the entire range of possible values of growth rates in a fire scenarios, i.e. the time at which the sprinklers activate for a fire with a growth rate of 0.04 kW/s<sup>2</sup> would also represent the time at which sprinklers activate for a fire with a growth rate of 0.06 kW/s<sup>2</sup> or 0.01 kW/s<sup>2</sup>, this simplification is done due the large computational time that would mean to evaluate every possible value of growth rate. Table 11 shows the representative values and the represented values of growth rates and the activation times.

Representative $\alpha$ (kW/s <sup>2</sup> )	Represented values of $\alpha$ (kW/s <sup>2</sup> )	Activation time (s)
0.04	0.0 - 0.06	100.01329
0.08	0.06 - 0.10	70.024216
0.12	0.10 - 0.14	60.022195
0.18	0.14 - 0.20	50.020154

Table 11: Growth rate values and activation times for sprinkler system

The resulting value for the activation time will determine the maximum values for HRR for the sprinkler case scenario. This is obtained by the t-squared fire formula, shown in equation 17.

$$\dot{Q} = \alpha \cdot t^2 \quad (17)$$

This resulting HRR will then remain constant thought the simulations and will be delimited by the maximum area, meaning that the values of HRRPUA will be maintained as the original values obtained by the Sobol sequence.

All input values, except the growth rates that will vary according to table 11, for the CFD simulations to determine the activation times for sprinklers remain constant are shown in table 12.

HRRPUA	AREA	HOC	CO yield
kW/m <sup>2</sup>	m <sup>2</sup>	kJ/kg	g/g
392.2323	4	25000	0.09

Table 12: Input values for CFD calculations of activation times for sprinklers

The maximum allowable distance between sprinkler heads for these type of locations is carried out according to [33], resulting then in the maximum possible distance of a sprinkler regardless the location of the fire would be 2.3 meters, at this distance the temperature is measured. One sprinkler and the devices locations is presented in figure 16, the rest of the sprinklers would be evenly distributed over the enclosure following the regulations presented in [33].

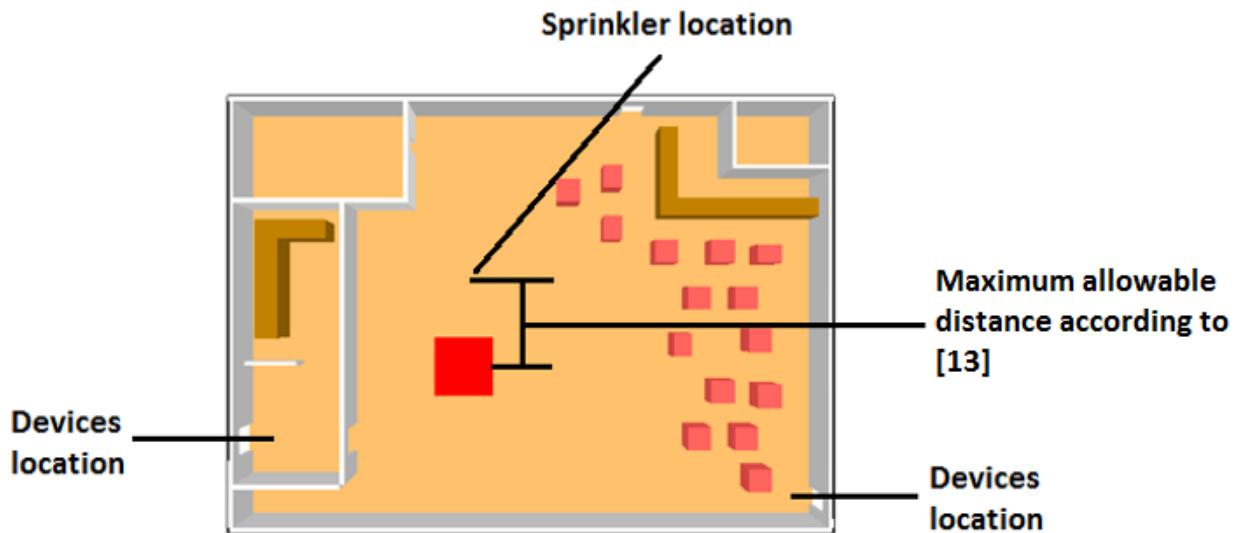


Figure 16: Sprinkler location according to [32]

These sprinkler activation times may not be on the conservative side, since the time that the smoke layer takes to heat up the sprinkler bulb itself is not taken into account, 3 different CFD scenarios were executed with a time delay of 30 more seconds that the times shown in table 11 representing the  $\alpha$  of 0.04, 0.06 and 0.12 to demonstrate that the temperature difference is small (around 10 to 20 °C over the 10 minutes of the simulation) between the chosen values for the CFD calculations in table 11 and the delayed activation times for the sprinklers as it would be more realistic. The results for these CFD test is shown in appendix A.

### 3.2.4. Case 4: Bar with extraction system

The layout for the fourth case of study is the same as described in section 3.2.2. An extraction system is added to the concept. The extraction rate will be a fixed value of  $10 \text{ m}^3/\text{s}$ . There is no calculation carried out to arrive to this value, the objective here is to observe the influence of the system over the output not to design a functional SHC system. The activation of the SHC is carried out in the same manner as the one presented in section 3.2.3, but instead of observing when the activation temperature is reached, the system will now activate when the smoke layer height start to descend, these times are displayed in table 13.

Representative $\alpha$ ( $\text{kW}/\text{s}^2$ )	Represented values of $\alpha$ ( $\text{kW}/\text{s}^2$ )	Activation time (s)
0.04	0.0 - 0.06	90.010713
0.08	0.06 - 0.10	60.022196
0.12	0.10 - 0.14	50.026016
0.18	0.14 - 0.20	40.007305

Table 13: Growth rate values and activation times for extraction system

46 extractors are evenly distributed over the enclosure, Figure 17 presents this distribution. The location of the main exit can be considered as a different smoke reservoir regarding the location of the fire and it appears that the extraction of smoke at this point works much better than at the section where the fire is located.

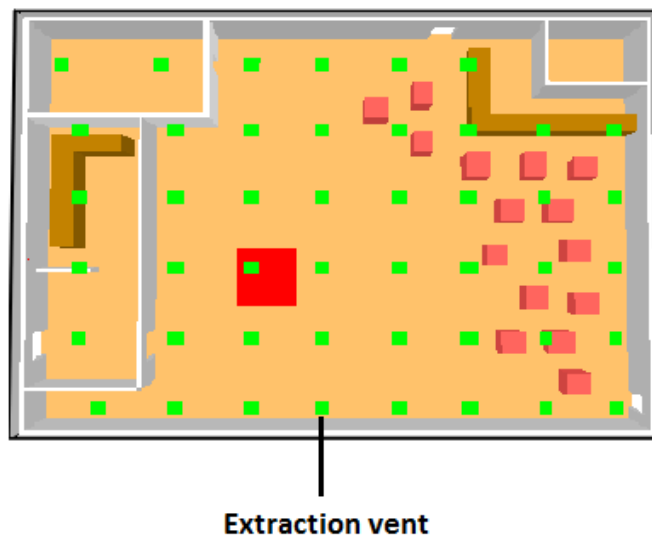


Figure 17: Extraction vent distribution

### 3.2.5. Case 5: Bar ventilation-controlled fire

For every case previously described the fire source is fuel-controlled meaning that it has enough provision of air coming in from its sides to generate as much HRR as the fuel allows it. For this case the fire source will be located inside a room with only one opening resulting in a ventilation-controlled fire delimited by the enclosure opening. The layout is the same as described in section 3.2.2, with the fire located inside the storage room as seen in figure 18.

The limiting factors for the area of the fire will be:

1. The area of the enclosure itself.
2. The values obtained from the Sobol quasi-random sequence.
3. The opening factor presented in equation 18, delimitating the maximum HRR for a ventilated-controlled fire.

$$\dot{Q} = 1500 A_o H_o^{1/2} \quad (18)$$

Where:

$A_o$  = area of the opening.

$H_o$  = height of the opening.

The value that produces the smallest HRR would then be the limiting factor for the area of the fire.

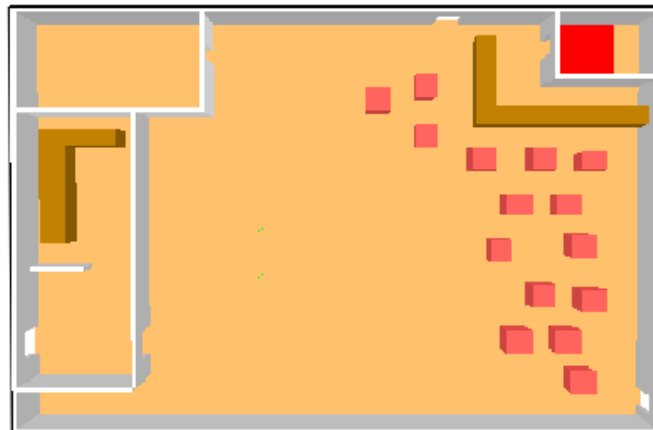


Figure 18: Ventilation-controlled fire

The dimensions of the room opening is 0.8 m width and 2 m height, the rest of the openings/exits remains as described in table 10.

## 4. Results

All resulting matrixes for the input parameters from Sobol quasi-random sequence and radial trajectories are presented in appendix B tables B.1 to B.4.

The output of the fire scenarios for the retail shop case is measured in 2 egress routes: at the main exit and at exit 2 (figures 13 and 14).

The output of fire scenarios for the bar cases 2, 3, 4 and 5, is measured in 2 egress routes: at the main exit and at exit 1 (figure 15).

The time step for the CFD and zone model simulations is 1 for every 10 seconds.

Two types of results are presented for each case:

1. The  $\mu^*$  and  $\sigma$  presented in graphs. Each graph shows the weight of all input parameters over the output, the interaction with other factors and/or a nonlinear behavior. The figures show three averages of the results over 300 – 400 s, 400 – 500 s and 500 – 600 s. This is done because at the early stages of the fire the only parameter influencing the output is the growth rate of the fire itself. Each parameter will be identified a specific color and the time in which is averaged is presented as a figure, according to figures 19 and 20.



Figure 19: Color identification of parameters

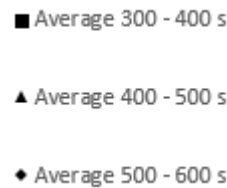


Figure 20: Time averages

2. The sensitivity index as an alternative approach to analyze the model behavior. The result presented is the average between 300 – 600 s of each parameter for the same reason described above.

The following results are for the main exits of each scenario, for the auxiliary exits results see Appendix C.

## 4.1. Case 1: Retail shop

### 4.1.1. Resulting $\mu^*$ and $\sigma$ at main exit shown in figures 21 – 24:

- Figures 21 and 22 shows the behavior of the input parameters both in FDS and CFAST for temperature. The growth rate of the fire plays the most important role presenting high influence on the output and interactions with other factors and/or nonlinear behavior increasing its influence as time goes by. The HRR of the fire gains influence over the output, this is reflected in an increasing importance of the area of the fuel. The diameter and flame height have a direct influence on the radiative heat fluxes and on the air entrainment which in consequence heats up the smoke layer [29], for locations far away from the fire source the heat is transported mostly by the smoke layer re-radiating back to the smoke free layer.

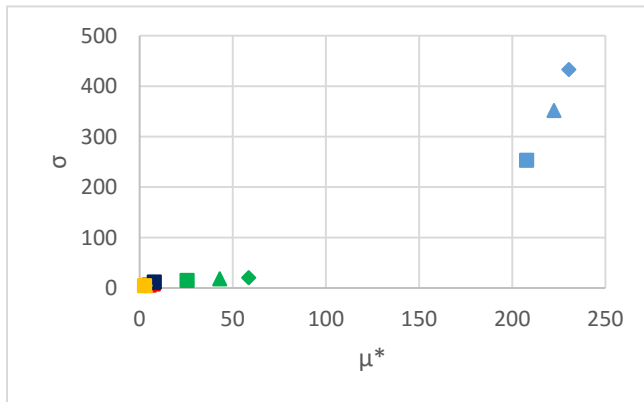


Figure 21: FDS results  $\mu^*$  and  $\sigma$ . Temperature main exit

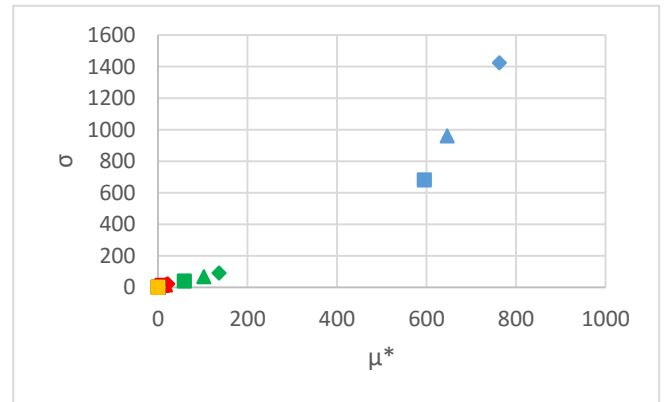


Figure 22: CFAST results  $\mu^*$  and  $\sigma$ . Temperature main exit

- Figures 23 and 24 shows the behavior of the input parameters both in FDS and CFAST for CO levels. Results show almost the same behavior as the temperature output, with the difference that the input parameter for the CO-yield appears to have a higher influence over the output, this as a results that the CO-yield levels are directly related with the CO production of the fire.

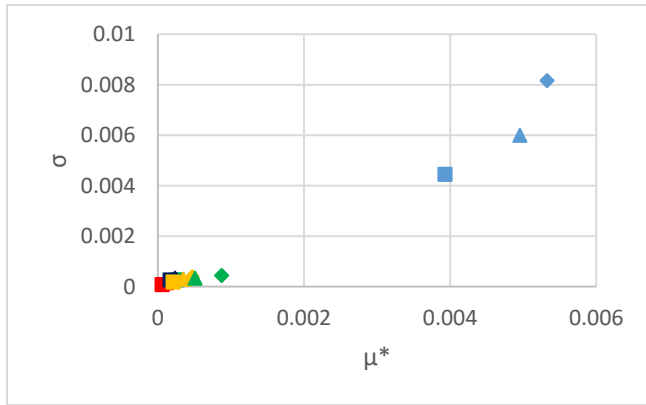


Figure 23: FDS results  $\mu^*$  and  $\sigma$ . CO levels main exit

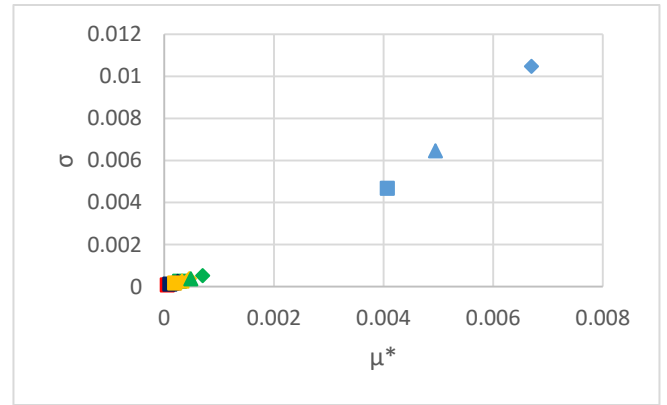


Figure 24: CFAST results  $\mu^*$  and  $\sigma$ . CO levels main exit upper layer

#### 4.1.2. Total sensitivity index results at main exit shown in tables 14 – 15:

- Tables 14 and 15 presents the results for the sensitivity index for both FDS and CFAST. The area of the fire appears to have a higher influence over the temperature and the CO-levels, but overall the most influential parameters are, as discussed in section 4.1.1, the growth rate of the fire, the area of the fuel and the CO-yield for the CO-levels output.

Output	Sti $\alpha$ %	Sti HRRPUA %	Sti Area %	Sti HOC %	Sti CO-yield %
Temperature	34.32%	2.83%	62.34%	0.21%	0.30%
CO levels	26.48%	2.14%	46.40%	2.10%	22.88%

Table 14: FDS results. Total sensitivity index main exit

Output	Sti $\alpha$ %	Sti HRRPUA %	Sti Area %	Sti HOC %	Sti CO-yield %
Temperature	40.90%	1.80%	57.30%	0.00%	0.00%
CO levels upper layer	32.17%	2.76%	44.43%	1.30%	19.33%

Table 15: CFAST results. Total sensitivity index main exit

## 4.2. Case 2: Bar

### 4.2.1. Resulting $\mu^*$ and $\sigma$ at main exit shown in figures 25 – 28:

- Figures 25 and 26 shows the behavior of the input parameters both in FDS and CFAST for temperature. The growth rate of the fire is the most influential parameter during the early stages. The HRR of the fire gains influence over time reflected as HRRPUA. The temperature of the areas surrounding the fire is affected mostly by the radiation from the fire source, different from large areas as the surroundings are heated mostly by the re-radiation from smoke layer.

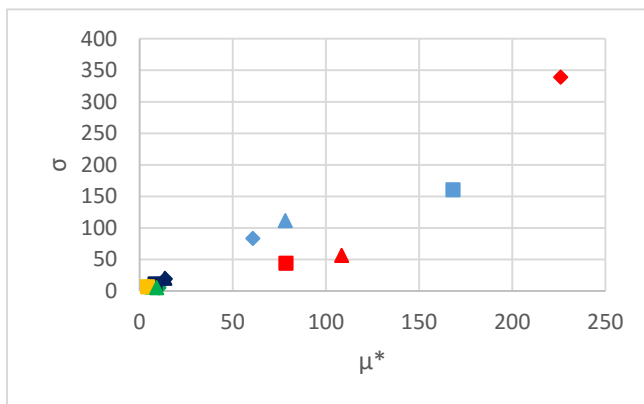


Figure 25: FDS results  $\mu^*$  and  $\sigma$ . Temperature main exit

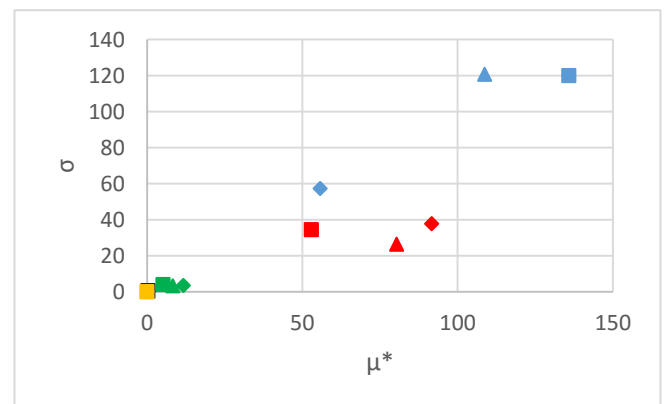


Figure 26: CFAST results  $\mu^*$  and  $\sigma$ . Temperature main exit

- Figures 27 and 28 shows the behavior of the input parameters both in FDS and CFAST for CO levels. FDS results present a similar behavior as the temperature where the growth rate of the fire is the most influential parameter in the early stages but over time the HRRPUA appears to take over, while the CO-yield has an effect over the output but it does not appear to have a non linear behavior or no interactions with the other parameters. CFAST presents that the only important parameter is the growth rate of the fire, this may be because the measures are given for the upper layer and not for fixed height as is in FDS, but nevertheless the HRRPUA appears to have some influence over the output.



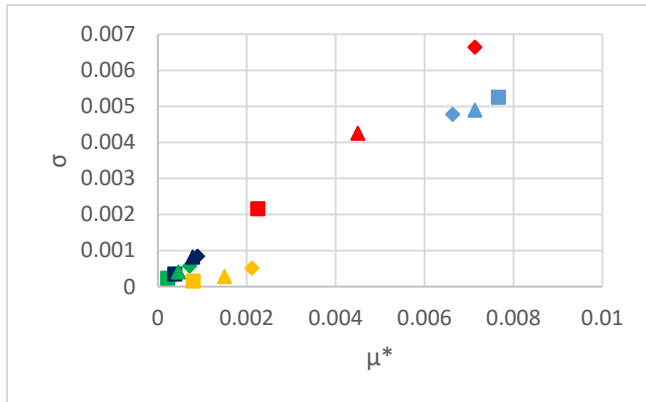


Figure 27: FDS results  $\mu^*$  and  $\sigma$ . CO levels main exit

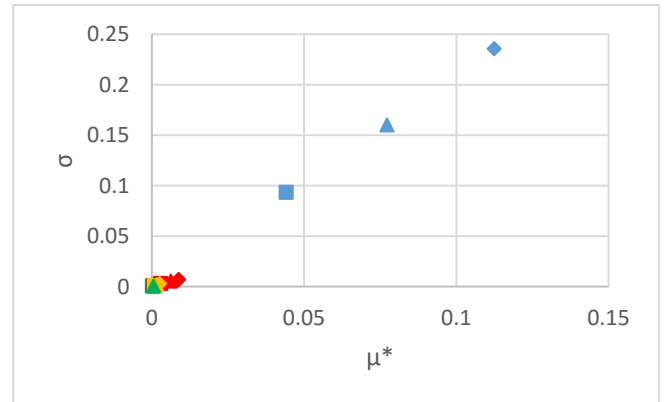


Figure 28: CFAST results  $\mu^*$  and  $\sigma$ . CO levels main exit upper layer

#### 4.2.2. Total sensitivity index results at main exit shown in tables 16 – 17:

- Tables 16 and 17 presents the results for the sensitivity index for both FDS and CFAST. For the FDS calculations the temperature appears to be highly influenced by the HRRPUA, follow by the CO-yield and then the growth rate of the fire, differing from the calculations in CFAST where the most important are the HRRPUA and the growth rate of the fire. The 3 input parameters should be taken into account as important. For the CO-levels FDS presents the HRRPUA as the most influential parameter while CFAST presents the growth rate of the fire, this may be because of the reason given in section 4.2.1 where the measurements in FDS are taken in a fixed height of 1.5 m, while CFAST analyzes the upper layer.

Output	Sti $\alpha$ %	Sti HRRPUA %	Sti Area %	Sti HOC %	Sti CO-yield %
Temperature	4.48%	72.27%	2.05%	2.84%	18.37%
CO levels	8.87%	74.85%	1.60%	1.61%	13.07%

Table 16: FDS results. Total sensitivity index main exit

Output	Sti $\alpha$ %	Sti HRRPUA %	Sti Area %	Sti HOC %	Sti CO-yield %
Temperature	11.65%	83.38%	4.85%	0.12%	0.00%
CO levels upper layer	75.54%	18.41%	0.79%	0.91%	4.34%

Table 17: CFAST results. Total sensitivity index main exit

### 4.3. Case 3: Bar with sprinkler system

#### 4.3.1. Resulting $\mu^*$ and $\sigma$ at main exit shown in figures 29 – 32:

- Figures 29 and 30 shows the behavior of the input parameters both in FDS and CFAST for temperature. The growth rate of the fire is the only parameter having any effect over the output and presenting a non linear behavior and/or having influence over the rest of the input parameters. The reason is that the sprinklers will act as a limiting factor over the HRR, not allowing it to fully develop in consequence the fire will not continue growing once the sprinklers activate, at which point none of the input parameters, other than the growth rate of the fire, appears to have any significant influence over the fire.

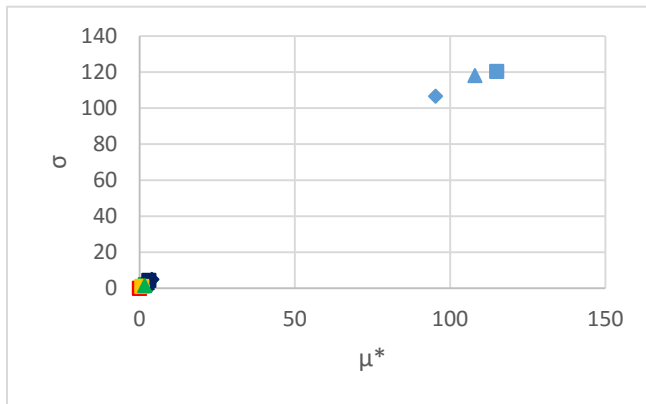


Figure 29: FDS results  $\mu^*$  and  $\sigma$ . Temperature main exit

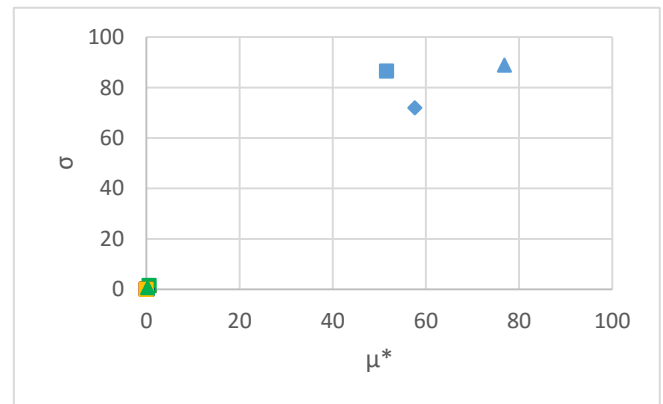


Figure 30: CFAST results  $\mu^*$  and  $\sigma$ . Temperature main exit

- Figures 30 and 31 shows the CO levels output for FDS and CFAST. FDS results presents the CO yield as the most influential parameter followed by the fire growth rate. CFAST results presents the growth rate of the fire followed by the heat of combustion as the most important parameters this may be as a consequence that maintaining a constant HRR and varying the heat of combustion would result in an increase or decrease of the pyrolyzate mass flow rate per unit area [29] and the fact that the measure is made for the upper layer not at 1.5 m.

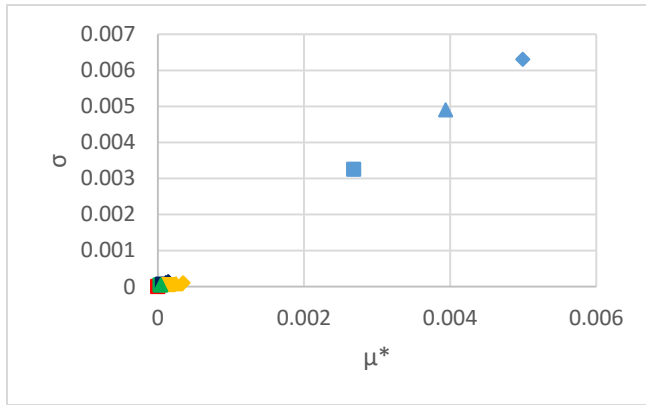


Figure 31: FDS results  $\mu^*$  and  $\sigma$ . CO levels main exit

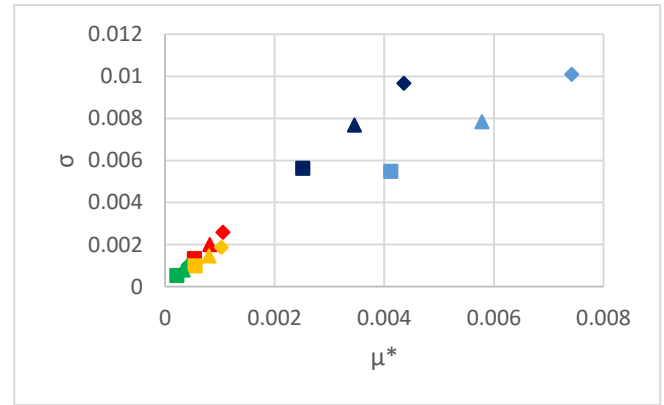


Figure 32: CFAST results  $\mu^*$  and  $\sigma$ . CO levels main exit upper layer

#### 4.3.2. Total sensitivity index results at main exit shown in tables 18 – 19:

- Tables 16 and 17 presents the results for the sensitivity index for both FDS and CFAST. It is clear that the temperature is only influenced by the growth rate of the fire as explained in section 4.3.1. For the CO levels FDS considers that the CO-yield as the most important parameter, while CFAST considers the HOC as the most influential one.

Output	St $\alpha$ %	St HRRPUA %	St Area %	St HOC %	St CO-yield %
Temperature	89.13%	0.00%	8.15%	1.60%	1.13%
CO levels	36.08%	0.00%	1.49%	1.68%	60.75%

Table 18: FDS results. Total sensitivity index main exit

Output	St $\alpha$ %	St HRRPUA %	St Area %	St HOC %	St CO-yield %
Temperature	93.75%	1.56%	4.29%	0.41%	0.00%
CO levels upper layer	8.17%	10.04%	10.40%	60.79%	10.59%

Table 19: CFAST results. Total sensitivity index main exit

## 4.4. Case 4: Bar with extraction system

### 4.4.1. Resulting $\mu^*$ and $\sigma$ at main exit shown in figures 33 – 36:

For this particular case the result vary greatly in both locations, this as a consequence of the influence of the extraction system over the enclosure where at the main exit seems to perform good, while at exit 1 it has little to no influence. For the results at exit 1 refer to appendix C.9 and C.10.

Main exit

- Figures 33 to 36 shows the output for both FDS and CFAST for temperature and CO levels. The effect of the extraction system will decrease the influence of every parameter, except the HRRPUA which will in consequence result as the most substantial parameter overall.

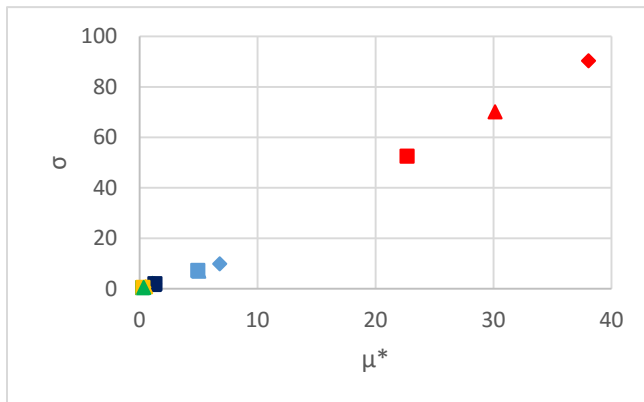


Figure 33: FDS results  $\mu^*$  and  $\sigma$ . Temperature main exit

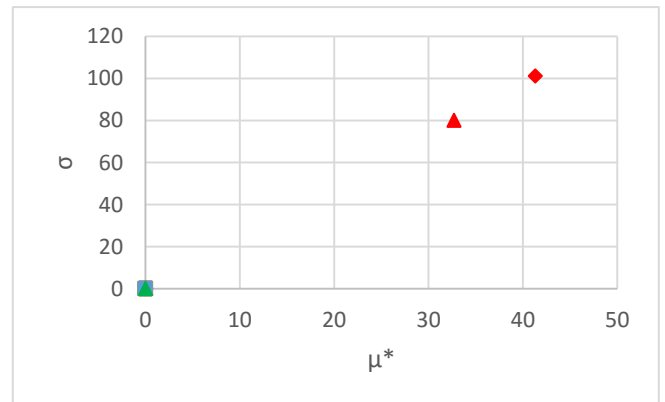


Figure 34: CFAST results  $\mu^*$  and  $\sigma$ . Temperature main exit

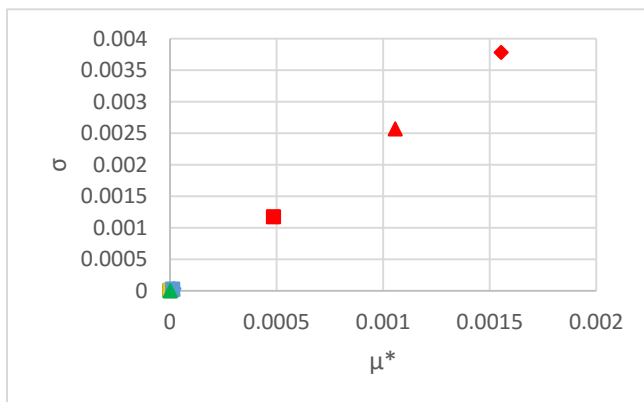


Figure 35: FDS results  $\mu^*$  and  $\sigma$ . CO levels main exit

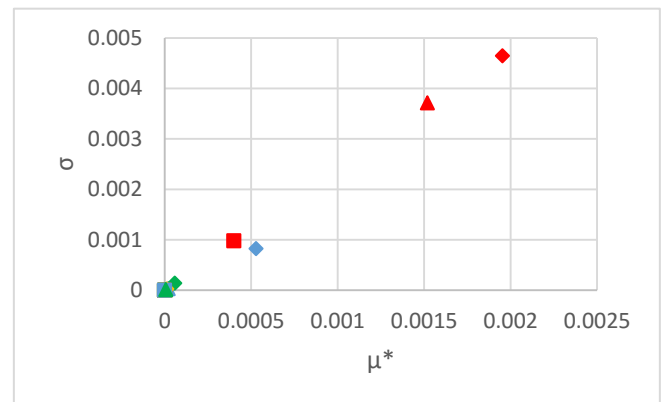


Figure 36: CFAST results  $\mu^*$  and  $\sigma$ . CO levels main exit upper layer

**4.4.2. Total sensitivity index results at main exit shown in tables 20 – 21:**

- Tables 20 and 21 presents the results for the sensitivity index for both FDS and CFAST. The behavior of the parameters is the same as the one discussed in section 4.4.1 (refer to section 4.4.1 for the discussion).

<b>Output</b>	<b>St <math>\alpha</math> %</b>	<b>St HRRPUA %</b>	<b>St Area %</b>	<b>St HOC %</b>	<b>St CO %</b>
Temperature	0.01%	99.96%	0.02%	0.01%	0.00%
CO levels	0.00%	100.00%	0.00%	0.00%	0.00%

**Table 20: FDS results. Total sensitivity index temperature main exit**

<b>Output</b>	<b>St <math>\alpha</math> %</b>	<b>St HRRPUA %</b>	<b>St Area %</b>	<b>St HOC %</b>	<b>St CO %</b>
Temperature	0.01%	99.97%	0.02%	0.00%	0.00%
CO levels upper layer	0.04%	99.92%	0.03%	0.00%	0.00%

**Table 21: CFAST results. Total sensitivity index temperature main exit**

**Exit 1**

Results are shown in the appendix sections C.9 and C.10, the discussion of the results is presented as follows:

- Temperature: the behavior is that as if the enclosure has no system acting upon it resulting in the HRRPUA and the fire growth as the most significant parameters. The CO-yield appears as the third most important parameter.
- CO levels: the HRRPUA is the most influential parameter increasing the influence over time as the growth rate decreases. For this case the CO-yield appears to have little influence.

## 4.5. Case 5: Bar ventilation-controlled fire

### 4.5.1. Resulting $\mu^*$ and $\sigma$ at main exit shown in figures 37 – 40:

- Figures 37 and 38 shows the behavior of the input parameters both in FDS and CFAST for temperature. The HRR increases its influence over time and the growth rate of the fire decreases. The HRRPUA appears to be the second most influential parameter. The area of the fuel shows an increase in importance on the effects over the output, the location of the fire source is at a greater distance, in comparison with the previous cases, relying in flame height to heat up the smoke layer to transport the heat to the devices location. Overall the growth rate of the fire is the most influential parameter.

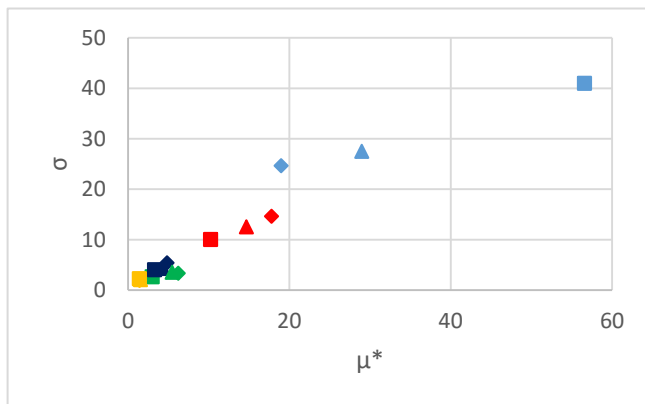


Figure 37: FDS results  $\mu^*$  and  $\sigma$ . Temperature main exit

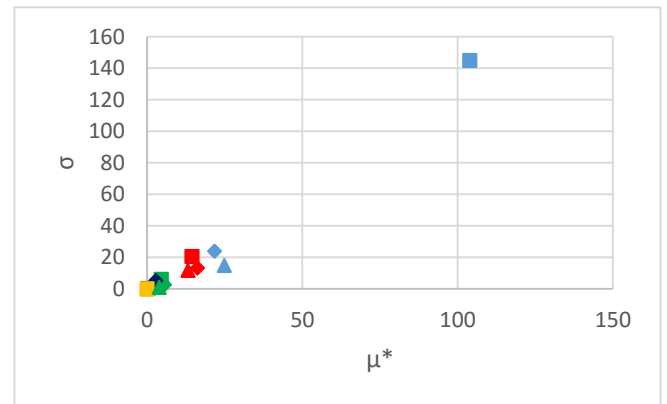


Figure 38: CFAST results  $\mu^*$  and  $\sigma$ . Temperature main exit

- Figures 39 and 40 shows the CO levels output for FDS. The behavior is similar to that of the temperature having the growth rate of the fire and the HRRPUA as the most important parameters. The CO-yield, HOC and the area appears to share the have similar influence over the fire, this may be regarded to the location of the fire source relevant to the location of the devices.

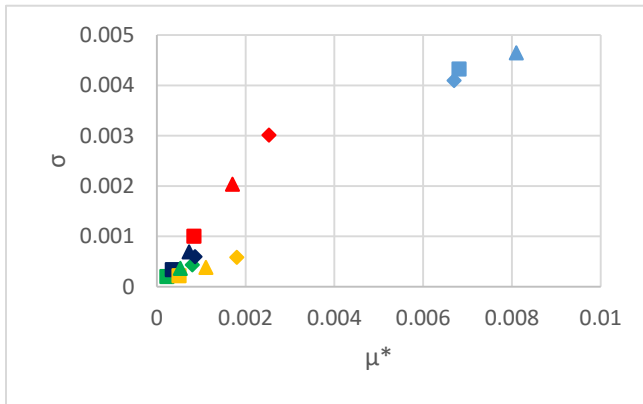


Figure 39: FDS results  $\mu^*$  and  $\sigma$ . CO levels main exit

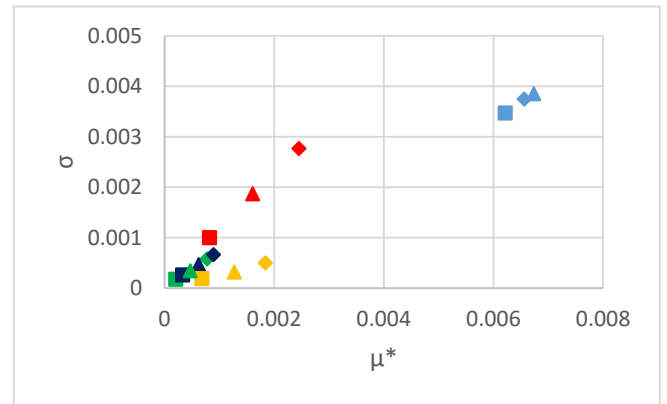


Figure 40: CFAST results  $\mu^*$  and  $\sigma$ . CO levels main exit upper layer

#### 4.5.2. Total sensitivity index results at main exit shown in tables 22 – 23:

- Tables 22 and 23 presents the results for the sensitivity index for both FDS and CFAST. The output of the temperature is similar as the one discussed in section 4.5.1. The CO levels seem to be highly affected by the CO-yield parameter, followed by the HRRPUA.

Output	St $\alpha$ %	St HRRPUA %	St Area %	St HOC %	St CO %
Temperature	16.03%	61.14%	18.47%	3.43%	0.93%
CO levels	21.19%	28.93%	7.27%	3.72%	38.90%

Table 22: FDS results. Total sensitivity index main exit

Output	St $\alpha$ %	St HRRPUA %	St Area %	St HOC %	St CO %
Temperature	19.58%	52.24%	15.23%	12.94%	0.00%
CO levels upper layer	14.29%	23.06%	6.82%	5.64%	50.19%

Table 23: CFAST results. Total sensitivity index main exit

## 5. Conclusions

A methodology to assess the impact of input parameters in fire scenario for life safety criteria is introduced. The focus is aimed to the physical parameters of fuel packages, specifically the HRRPUA, area of the fuel, growth rate of the fire, heat of combustion and CO-yield.

Fire simulations are carried out to evaluate the conditions within the fire enclosures with 2 different fire models FDS 6 and CFAST 7.1.1. 5 cases are evaluated each with 36 representative scenarios, resulting in 180 fire simulations per model. The method relies on 2 different approaches to compute sensitivity analyses: a screening method based on the calculation of the mean of the absolute values and standard deviation based on the elementary effect method and the estimation of the global sensitivity index.

Each case evaluated presents different conditions but overall, for enclosures with no fire protection systems, results suggest that the most influential parameters is the growth rate of the fire followed by the HRRPUA for enclosures with small dimensions and area of the fuel for enclosure with large dimensions.

The effects of input parameters for enclosures with sprinkler systems and SHC are evaluated. Provided that the systems work correctly, the HRRPUA and the area of the fire has little influence for enclosures protected by sprinkler systems, having the growth rate of the fire as the single most influential parameter. For enclosures protected by smoke extraction systems the only influential parameter is the HRRPUA.

Sensitivity analyses are specific for each fire scenario thus absolute conclusions cannot be drawn, different scenarios present different conditions and in consequence will present variations on the importance of the input parameters. For most of the cases, not all, growth rate of the fire and HRR appear to be the most significant parameters.



## 6. SUGGESTIONS

Considering that mainly the physical parameters of the fire were accounted for, it is important to further investigate:

- The influence of the parameters related to boundary conditions, such as the geometry of the enclosure, the location of the fire source, location of obstructions and openings of the enclosure.
- The uncertainty of the model employed to perform the fire model calculations, this may produce substantial variations over the output.
- Though fire models are an accurate representation of reality it would be good to make a real life test out some of these fire scenarios to compare the variations between them.
- The influence of the parameters over other parameters and the non linear behavior should be explored more in depth, since it is not clear when one or the other occurs when executing the elementary effect analysis.

## **7. Acknowledgements**

The author would like to show his gratitude to all the people involved in the entire master's programme.

Firstly to Bart Van Weyenberge my supervisor and co-promotor for the support and guidance in the elaboration of the thesis and experiments, and whom without this would have not been possible.

Secondly to Prof. Bart Merci for organizing such an exceptional programme.

Third to all my classmates and friends for all the great times we shared.

And last but not least to my family for all the unconditional support and encouragement that they have always demonstrated, my love always to you.

## 8. References

- [1] SFPE, Engineering guide to performance-based fire protection, 2006.
- [2] S. Kaplan and J. Garrick, "On the quantitative definition of risk," 1981.
- [3] International Risk Governance Council, 2006.
- [4] H. Frantzich, "Uncertainty and Risk Analysis in Fire Safety Engineering," Lund University, Lund, 1998.
- [5] ISO-31000, Risk management - Principles and guidelines, 2009.
- [6] H. Hassel, "Introduction to risk assessment," in *Risk assessment*, Lund, 2015.
- [7] H. Theler, "A general framework for risk assessment," 2013.
- [8] B. Van Weyenberge and X. Deckers, "Development of a risk assessment method for fire in rail tunnels," Ghent University, Ghent, 2014.
- [9] FIRE - tech WG6, European study into the Fire Risk to European Cultural Heritage, Research European Commission, 2003.
- [10] G. Apostolakis, "How useful is quantitative risk assessment?," *Risk Analysis*, Vol 24, 2004.
- [11] C. Albrecht, A risk-informed and performance-based life safety concept in case of fire, 2012.
- [12] H. Hassel, *Probabilities and frequencies*, Lund, 2015.
- [13] S. Jonkman, P. van Gelder and J. Vrijlin, "An overview of quantitative risk measures for loss of life and economic damage.," *Journal of Hazardous Materials*, 3 September 2003.
- [14] ISO 16732, Fire safety engineering - fire risk assessment ISO 16732 -, 2011.
- [15] M. Hurley and E. Rosenbaum, Performance-based fire safety design, 2015.
- [16] R. Gann and N. Bryner, "Combustion Products and Their Effects on Life Safety," in *Fire Protection Handbook*, Quincy, National Fire Protection Assoc., 2008, pp. Chapter 6, 11 - 34 .
- [17] NFPA, Fire Protection Handbook, Quincy: NFPA, 2003.

- [18] EPA, "Sensitivity Analysis: How Do We Know What's Important?," in *Risk Assessment Guidance for Superfund: Volume III - Part A, Process for Conducting Probabilistic Risk Assessment*, Washington DC, 2001, pp. Appendix A-1 - A-37.
- [19] A. Saltelli, M. Ratto, S. Tarantola and F. Campolongo, "Sensitivity Analysis for Chemical Models," Ispra, 2004.
- [20] F. Campolongo, A. Saltelli and J. Cariboni, "From screening to quantitative sensitivity analysis. A unified approach," *Computer Physics Communications*, pp. 978-988, 6 January 2011.
- [21] M. Morris, "Factorial Sampling Plans for Preliminary Computational Experiments," *Technometrics*, Vol 33, No 2, pp. 161-174, May 1991.
- [22] B. Van Weyenberge, X. Deckers, R. Caspeele and B. Merci, "Sensitivity analysis for QRA of life safety in case of fire," Ghent, 2016.
- [23] A. Saltelli, M. Ratto, T. Andres, F. Campolongo, J. Cariboni, D. Gatelli, M. Saisana and S. Tarantola, *Global Sensitivity Analysis*, UK: Wiley, 2008.
- [24] F. Campolongo, A. Saltelli and J. Cariboni, "An effective screening design for sensitivity analysis of large models," *Environmental Modelling & Software*, pp. 1509-1518, 18 January 2007.
- [25] F. Campolongo, J. Cariboni and A. saltelli, "An effective screening design for sensitivity analysis of large models.," *Environmental Modelling and Software*, vol. 22, pp. 1509-1518, 2007.
- [26] A. Saltelli, P. Annoni, A. C. F. Ivano, M. Ratto and S. Tarantola, "Variance based sensitivity analysis of model output. Design and estimator for the total sensitivity index," *Computer Physics Communications*, pp. 259-270, 2010.
- [27] J. Ribeiro and J. Carmona, "A Method for Assessing Parameter Impact on Control-Flow Discovery Algorithms," Universitat Politècnica de Catalunya, Barcelona.
- [28] A. Saltelli, M. Ratto, T. Andres, F. Campolongo, J. Cariboni, D. Gatelli, M. Saisana and S. Tarantola, *Global Sensitivity Analysis. The Primer*, Ispra: John Wiley & Sons, Ltd. , 2008.
- [29] J. Wolfram and G. T. J. Rein, "The effect of Model Parameters on the Simulation of Fire Dynamics," International association for fire science, Edinburgh, 2008.
- [30] UQLAB, *UQLAB: Uncertainty Quantification in MATLAB*, Zurich, 2011.

- [31] National Fire Protection Association, Guide for smoke and heat venting, Quincy: National Fire Protection Association, 1985.
- [32] D. Purser, "Toxic Hazards to Fire Figthers, Including Effects of Fire Retardants, During Fires and Post-Fire Investigation Activities," in *Toxic Hazards to Fire Figthers, Including Effects of Fire Retardants, During Fires and Post-Fire Investigation Activities*, Hatfield, 2009.
- [33] National Fire Protection Association, NFPA 13: Standard for the installation of Sprinkler Systems, National Fire Protection Association, 1999.
- [34] M. Morris, "Factorial sampling plans for preliminary computational experiments," *Technometrics*, vol. 33, pp. 161-174, 1991.
- [35] B. Karlsson and J. Quintiere, Enclosure fire dynamics, 2000.
- [36] S. Hansson, "Risk: objective or subjective facts or values," *Journal of Risk Research*, pp. 231-238, 2010.
- [37] International Standard Organization, ISO-31000, 2009.
- [38] H. Ingason, M. N. D. Kumm, A. Lönnermark, A. Claesson, Y. Z. Li, K. Fridolf, R. Åkerstedt, H. Nyman, T. Dittmer, R. Forsén, B. Janzon, G. Meyer, A. Bryntse, T. Carlberg, N.-E. L and A. Palm, The Metro Project - Final report, Sweden : Mälardalen University Press , 2012.

## APPENDIX A

Values of temperature obtained for sprinklers with extra activation time vs values obtained for sprinklers with activation times given by table 11.

Time	Temperature C activation at 100 s	Temperature C activation at 130 s	CO levels mol/mol activation at 100 s	CO levels mol/mol activation at 130 s
0	20	20	0	0
100	20.005932	20.013697	1.17169E-09	1.60923E-14
200	20.794661	24.8964	7.09149E-06	3.8832E-05
300	27.370398	35.562302	9.82379E-05	0.000218742
400	30.445288	37.154709	0.000201975	0.000380608
500	29.913216	36.018696	0.000278838	0.000502053
600	29.919573	36.436218	0.000358378	0.000629943

Table A.1 results  $\alpha$  0.04. Bar main exit

Time	Temperature C activation at 100 s	Temperature C activation at 130 s	CO levels mol/mol activation at 100 s	CO levels mol/mol activation at 130 s
0	20	20	0	0
100	24.732155	24.014843	4.11063E-05	3.21962E-05
200	47.094612	63.370846	0.000295311	0.000467972
300	47.097694	78.07151	0.000402141	0.000694234
400	54.635815	72.487244	0.00052064	0.000842216
500	51.735275	76.083603	0.000587305	0.000972735
600	51.485123	74.008385	0.000655737	0.001064978

Table A.2 results  $\alpha$  0.04. Bar exit 1

Time	Temperature C activation at 70 s	Temperature C activation at 100 s	CO levels mol/mol activation at 70 s	CO levels mol/mol activation at 100 s
0	20	20	0	0
100	20.004684	20.010296	2.76238E-14	1.94825E-19
200	20.330418	21.291992	3.08345E-06	9.10664E-06
300	26.505287	32.011925	7.74351E-05	0.000158351
400	27.909174	34.169827	0.0001443	0.000281027
500	29.390884	33.622524	0.000227728	0.000381672
600	29.30364	33.239628	0.000298864	0.000485342

Table A.3 results  $\alpha$  0.08. Bar main exit

Time	Temperature C activation at 70 s	Temperature C activation at 100 s	CO levels mol/mol activation at 70 s	CO levels mol/mol activation at 100 s
0	20	20	0	0
100	23.664557	22.162952	3.04526E-05	1.71846E-05
200	43.514664	52.009991	0.000253547	0.000351541
300	46.763176	63.13311	0.000357242	0.000539259
400	49.667194	67.589905	0.000442505	0.000661386
500	51.315739	65.673462	0.000513295	0.000727662
600	49.433559	64.639168	0.000555944	0.000819441

Table A.4 results  $\alpha$  0.08. Bar exit 1

Time	Temperature C activation at 60 s	Temperature C activation at 90 s	CO levels mol/mol activation at 60 s	CO levels mol/mol activation at 90 s
0	20	20	0	0
100	20.042788	20.233727	1.05873E-07	7.51755E-07
200	23.893574	33.343037	3.47034E-05	0.000125664
300	28.639568	39.635719	0.000121709	0.000324025
400	30.552729	39.650097	0.000216671	0.000514931
500	31.349764	39.316685	0.000308353	0.000659385
600	31.799477	39.670635	0.00038702	0.00080533

Table A.5 results  $\alpha$  0.12. Bar main exit

Time	Temperature C activation at 60 s	Temperature C activation at 90 s	CO levels mol/mol activation at 60 s	CO levels mol/mol activation at 90 s
0	20	20	0	0
100	29.401493	36.17696	8.87945E-05	0.000141471
200	50.678646	73.772133	0.00034451	0.000608935
300	51.576508	87.420563	0.000442383	0.000882377
400	55.205379	88.665733	0.000540421	0.001042531
500	56.683125	86.69828	0.000615951	0.001176213
600	54.412975	85.033066	0.000692991	0.001303938

Table A.6 results  $\alpha$  0.12. Bar exit 1

## APPENDIX B

Resulting tables from the Sobol quasi-random sequence for all cases:

$\alpha$	HRRPUA	Area	HOC	CO-yield
kW/s <sup>2</sup>	kW/m <sup>2</sup>	m <sup>2</sup>	kJ/kg	g/g
0.02152456	392.23227	2.29331874	25000	0.09
0.01787635	392.23227	2.29331874	25000	0.09
0.02152456	417.781359	2.29331874	25000	0.09
0.02152456	392.23227	0.19558745	25000	0.09
0.02152456	392.23227	2.29331874	26274.5575	0.09
0.02152456	392.23227	2.29331874	25000	0.07725443
0.01526715	448.286091	0.54150225	27697.959	0.06302041
0.01248214	448.286091	0.54150225	27697.959	0.06302041
0.01526715	380.200991	0.54150225	27697.959	0.06302041
0.01526715	448.286091	3.21120053	27697.959	0.06302041
0.01526715	448.286091	0.54150225	28548.5862	0.06302041
0.01526715	448.286091	0.54150225	27697.959	0.10955106
0.03670087	343.187435	9.71244512	22302.041	0.11697959
0.02396971	343.187435	9.71244512	22302.041	0.11697959
0.03670087	531.484906	9.71244512	22302.041	0.11697959
0.03670087	343.187435	0.08603355	22302.041	0.11697959
0.03670087	343.187435	9.71244512	23044.8944	0.11697959
0.03670087	343.187435	9.71244512	22302.041	0.05451414
0.01329798	417.781359	26.8898172	29601.3975	0.10274557
0.04507117	417.781359	26.8898172	29601.3975	0.10274557
0.01329798	329.034212	26.8898172	29601.3975	0.10274557
0.01329798	417.781359	0.80575019	29601.3975	0.10274557
0.01329798	417.781359	26.8898172	18863.5178	0.10274557
0.01329798	417.781359	26.8898172	29601.3975	0.15136482
0.02705779	312.32255	1.15964249	23725.4425	0.04398602
0.0164729	312.32255	1.15964249	23725.4425	0.04398602
0.02705779	432.098057	1.15964249	23725.4425	0.04398602
0.02705779	312.32255	15.3098075	23725.4425	0.04398602
0.02705779	312.32255	1.15964249	25629.2427	0.04398602
0.02705779	312.32255	1.15964249	23725.4425	0.08370757
0.01787635	368.245616	4.53528642	20398.6025	0.13601398
0.01421878	368.245616	4.53528642	20398.6025	0.13601398
0.01787635	289.464766	4.53528642	20398.6025	0.13601398
0.01787635	368.245616	61.1309305	20398.6025	0.13601398



0.01787635	368.245616	4.53528642	21451.4138	0.13601398
0.01787635	368.245616	4.53528642	20398.6025	0.02863518

Table B.1: Resulting matrix from Sobol sequence for case 2 and 4: Bar and bar with extraction system

$\alpha$	HRRPUA	Area	HOC	CO-yield
kW/s <sup>2</sup>	kW/m <sup>2</sup>	m <sup>2</sup>	kJ/kg	g/g
0.05072573	392.23227	6.86634935	25000	0.09
0.03975837	392.23227	6.86634935	25000	0.09
0.05072573	392.23227	9.85667756	25000	0.09
0.05072573	312.32255	6.86634935	25000	0.09
0.05072573	392.23227	6.86634935	26274.5575	0.09
0.05072573	392.23227	6.86634935	25000	0.07725443
0.03228893	343.187435	15.4188987	27697.959	0.06302041
0.02471423	343.187435	15.4188987	27697.959	0.06302041
0.03228893	343.187435	5.83879638	27697.959	0.06302041
0.03228893	404.644274	15.4188987	27697.959	0.06302041
0.03228893	343.187435	15.4188987	28548.5862	0.06302041
0.03228893	343.187435	15.4188987	27697.959	0.10955106
0.10146116	448.286091	3.74974155	22302.041	0.11697959
0.05837997	448.286091	3.74974155	22302.041	0.11697959
0.10146116	448.286091	51.7613729	22302.041	0.11697959
0.10146116	289.464766	3.74974155	22302.041	0.11697959
0.10146116	448.286091	3.74974155	23044.8944	0.11697959
0.10146116	448.286091	3.74974155	22302.041	0.05451414
0.02688695	492.587403	9.85667756	29601.3975	0.10274557
0.13220687	492.587403	9.85667756	29601.3975	0.10274557
0.02688695	492.587403	3.26494718	29601.3975	0.10274557
0.02688695	356.04454	9.85667756	29601.3975	0.10274557
0.02688695	492.587403	9.85667756	18863.5178	0.10274557
0.02688695	492.587403	9.85667756	29601.3975	0.15136482
0.06835925	368.245616	2.85031115	23725.4425	0.04398602
0.03569888	368.245616	2.85031115	23725.4425	0.04398602
0.06835925	368.245616	12.1457983	23725.4425	0.04398602
0.06835925	467.568867	2.85031115	23725.4425	0.04398602
0.06835925	368.245616	2.85031115	25629.2427	0.04398602
0.06835925	368.245616	2.85031115	23725.4425	0.08370757
0.03975837	417.781359	5.00741543	20398.6025	0.13601398
0.02938614	417.781359	5.00741543	20398.6025	0.13601398
0.03975837	417.781359	2.49253709	20398.6025	0.13601398
0.03975837	531.484906	5.00741543	20398.6025	0.13601398
0.03975837	417.781359	5.00741543	21451.4138	0.13601398

0.03975837	417.781359	5.00741543	20398.6025	0.02863518
------------	------------	------------	------------	------------

Table B.2: Resulting matrix from Sobol sequence for case 2 and 4: Bar and bar with extraction system

$\alpha$	HRRPUA	Area	HOC	CO-yield
kW/s <sup>2</sup>	kW/m <sup>2</sup>	m <sup>2</sup>	kJ/kg	g/g
0.05072573	392.23227	1.29360118	25000	0.09
0.03975837	392.23227	1.01391306	25000	0.09
0.05072573	392.23227	1.29360118	25000	0.09
0.05072573	312.32255	1.62457731	25000	0.09
0.05072573	392.23227	1.29360118	26274.5575	0.09
0.05072573	392.23227	1.29360118	25000	0.07725443
0.03228893	343.187435	0.94110424	27697.959	0.06302041
0.02471423	343.187435	0.72032943	27697.959	0.06302041
0.03228893	343.187435	0.94110424	27697.959	0.06302041
0.03228893	404.644274	0.79817057	27697.959	0.06302041
0.03228893	343.187435	0.94110424	28548.5862	0.06302041
0.03228893	343.187435	0.94110424	27697.959	0.10955106
0.10146116	448.286091	0.81539548	22302.041	0.11697959
0.05837997	448.286091	1.30263886	22302.041	0.11697959
0.10146116	448.286091	0.81539548	22302.041	0.11697959
0.10146116	289.464766	1.26278046	22302.041	0.11697959
0.10146116	448.286091	0.81539548	23044.8944	0.11697959
0.10146116	448.286091	0.81539548	22302.041	0.05451414
0.02688695	492.587403	0.54597619	29601.3975	0.10274557
0.13220687	492.587403	0.96692872	29601.3975	0.10274557
0.02688695	492.587403	0.54597619	29601.3975	0.10274557
0.02688695	356.04454	0.75535772	29601.3975	0.10274557
0.02688695	492.587403	0.54597619	18863.5178	0.10274557
0.02688695	492.587403	0.54597619	29601.3975	0.15136482
0.06835925	368.245616	0.91024057	23725.4425	0.04398602
0.03569888	368.245616	0.96968889	23725.4425	0.04398602
0.06835925	368.245616	0.91024057	23725.4425	0.04398602
0.06835925	467.568867	0.71688285	23725.4425	0.04398602
0.06835925	368.245616	0.91024057	25629.2427	0.04398602
0.06835925	368.245616	0.91024057	23725.4425	0.08370757
0.03975837	417.781359	0.95190801	20398.6025	0.13601398
0.02938614	417.781359	0.70357257	20398.6025	0.13601398
0.03975837	417.781359	0.95190801	20398.6025	0.13601398
0.03975837	531.484906	0.74826099	20398.6025	0.13601398
0.03975837	417.781359	0.95190801	21451.4138	0.13601398

0.03975837	417.781359	0.95190801	20398.6025	0.02863518
------------	------------	------------	------------	------------

Table B.3: Resulting matrix from Sobol sequence for case 3: Bar with sprinkler system

$\alpha$	HRRPUA	Area	HOC	CO-yield
kW/s <sup>2</sup>	kW/m <sup>2</sup>	m <sup>2</sup>	kJ/kg	g/g
0.05072573	392.23227	6.25	25000	0.09
0.03975837	392.23227	6.25	25000	0.09
0.05072573	392.23227	6.25	25000	0.09
0.05072573	312.32255	6.25	25000	0.09
0.05072573	392.23227	6.25	26274.5575	0.09
0.05072573	392.23227	6.25	25000	0.07725443
0.03228893	343.187435	6.25	27697.959	0.06302041
0.02471423	343.187435	6.25	27697.959	0.06302041
0.03228893	343.187435	5.83879638	27697.959	0.06302041
0.03228893	404.644274	6.25	27697.959	0.06302041
0.03228893	343.187435	6.25	28548.5862	0.06302041
0.03228893	343.187435	6.25	27697.959	0.10955106
0.10146116	448.286091	3.74974155	22302.041	0.11697959
0.05837997	448.286091	3.74974155	22302.041	0.11697959
0.10146116	448.286091	6.25	22302.041	0.11697959
0.10146116	289.464766	3.74974155	22302.041	0.11697959
0.10146116	448.286091	3.74974155	23044.8944	0.11697959
0.10146116	448.286091	3.74974155	22302.041	0.05451414
0.02688695	492.587403	6.25	29601.3975	0.10274557
0.13220687	492.587403	6.25	29601.3975	0.10274557
0.02688695	492.587403	3.26494718	29601.3975	0.10274557
0.02688695	356.04454	6.25	29601.3975	0.10274557
0.02688695	492.587403	6.25	18863.5178	0.10274557
0.02688695	492.587403	6.25	29601.3975	0.15136482
0.06835925	368.245616	2.85031115	23725.4425	0.04398602
0.03569888	368.245616	2.85031115	23725.4425	0.04398602
0.06835925	368.245616	6.25	23725.4425	0.04398602
0.06835925	467.568867	2.85031115	23725.4425	0.04398602
0.06835925	368.245616	2.85031115	25629.2427	0.04398602
0.06835925	368.245616	2.85031115	23725.4425	0.08370757
0.03975837	417.781359	5.00741543	20398.6025	0.13601398
0.02938614	417.781359	5.00741543	20398.6025	0.13601398
0.03975837	417.781359	2.49253709	20398.6025	0.13601398
0.03975837	531.484906	5.00741543	20398.6025	0.13601398
0.03975837	417.781359	5.00741543	21451.4138	0.13601398

0.03975837	417.781359	5.00741543	20398.6025	0.02863518
------------	------------	------------	------------	------------

**Table B.4: Resulting matrix from Sobol sequence for case 4: Bar ventilation-controlled fire**

## APPENDIX C

### C.1. Resulting $\mu^*$ and $\sigma$ retail shop at exit 2 shown in figures C.1.1 – C.1.4:

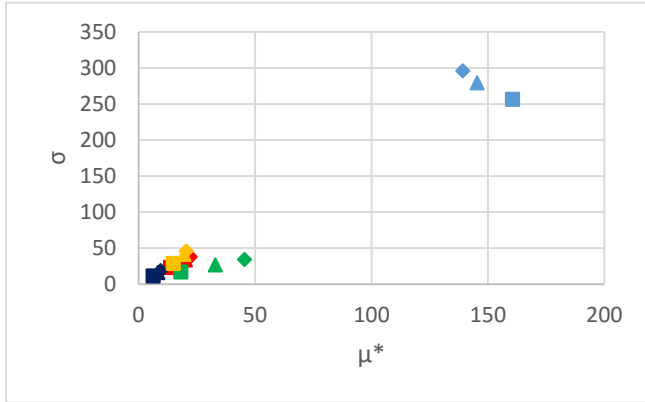


Figure C.1.1: FDS results. Temperature exit 1

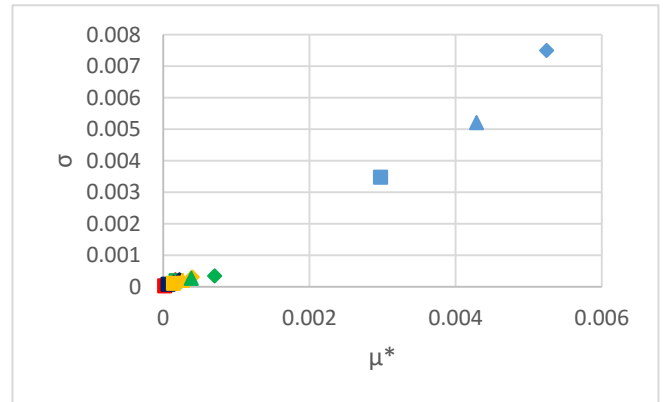


Figure C.1.2: FDS results. CO levels exit 1

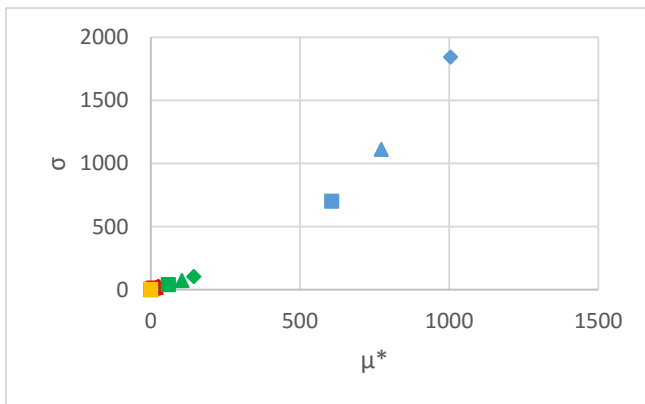


Figure C.1.3: CFAST results. Temperature exit 1

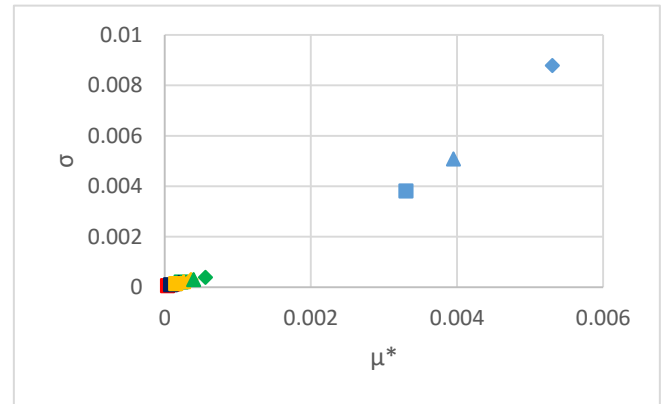


Figure C.1.4: CFAST results. CO levels exit 1 upper layer

### C.2. Total sensitivity index results retail shop at exit 2 tables C.2.1 – C.2.2:

Output	St $\alpha$ %	St HRRPUA %	St Area %	St HOC %	St CO %
Temperature	12.80%	22.75%	36.35%	13.31%	14.79%
CO levels	30.34%	3.20%	44.93%	1.31%	20.22%

Table C.2.1: FDS results. Total sensitivity index exit 2

Output	St $\alpha$ %	St HRRPUA %	St Area %	St HOC %	St CO %
Temperature	45.35%	1.73%	52.92%	0.00%	0.00%
CO levels upper layer	33.19%	2.72%	43.74%	1.23%	19.12%

Table C.2.2: CFAST results. Total sensitivity index exit 2

**C.3. Resulting  $\mu^*$  and  $\sigma$  bar at exit 1 shown in figures C.3.1 – C.3.4:**

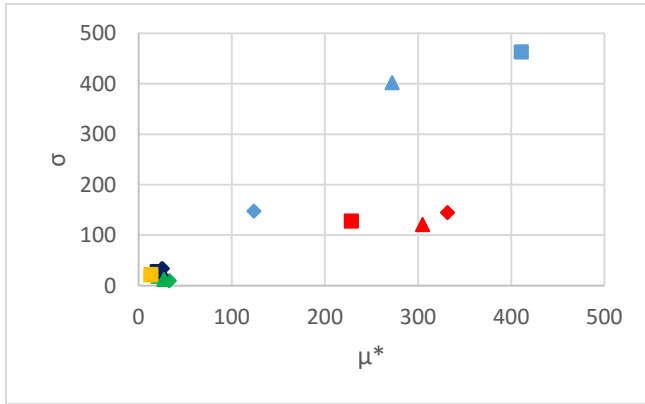


Figure C.3.1: FDS results. Temperature exit 1

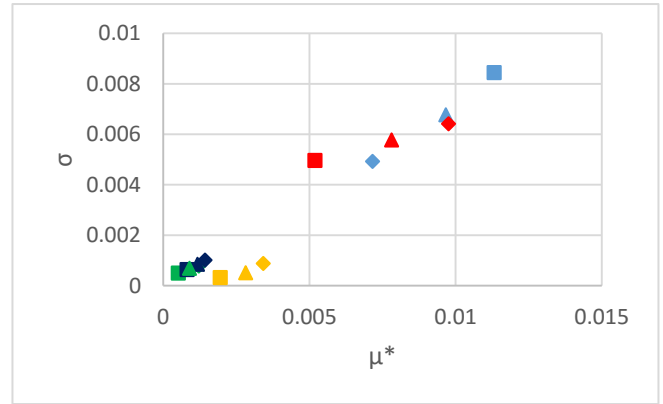


Figure C.3.1: FDS results. CO levels exit 1

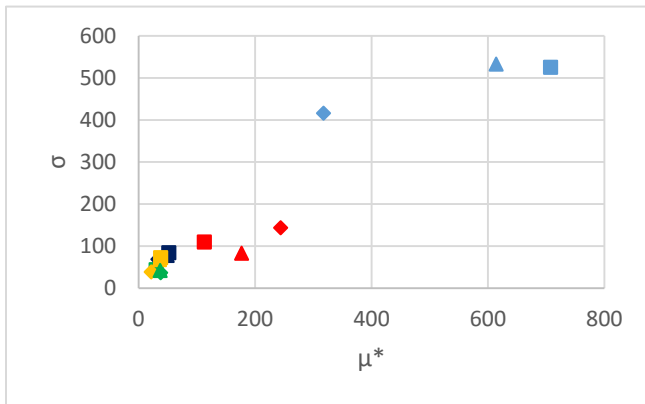


Figure C.3.3: CFAST results. Temperature exit 1

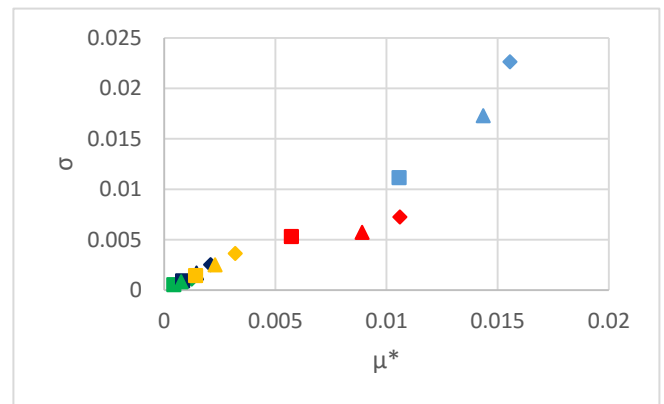


Figure C.3.4: CFAST results. CO levels exit 1 upper layer

**C.4. Total sensitivity index results bar at exit 1 tables C.4.1 – C.4.2:**

Output	St $\alpha$ %	St HRRPUA %	St Area %	St HOC %	St CO %
--------	---------------	-------------	-----------	----------	---------

Temperature	4.59%	91.64%	2.89%	0.14%	0.73%
CO levels	4.48%	72.27%	2.05%	2.84%	18.37%

Table C.4.1: FDS results. Total sensitivity index exit 1

Output	St $\alpha$ %	St HRRPUA %	St Area %	St HOC %	St CO %
Temperature	14.80%	61.54%	10.10%	6.81%	6.76%
CO levels	7.77%	57.56%	3.49%	5.95%	25.23%

Table C.4.2: CFAST results. Total sensitivity index exit 1

**C.5. Resulting  $\mu^*$  and  $\sigma$  bar with sprinkler system at exit 1 shown in figures C.5.1 – C.5.4:**

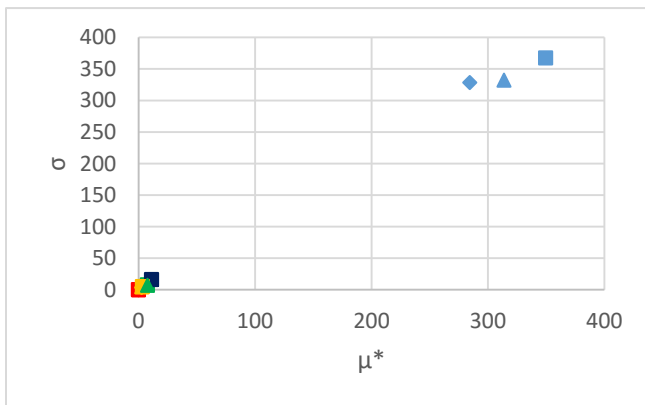


Figure C.5.1: FDS results. Temperature exit 1

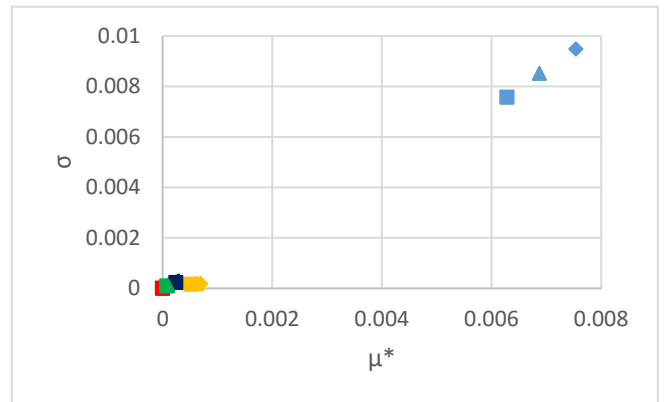


Figure C.5.2: FDS results. CO levels exit 1

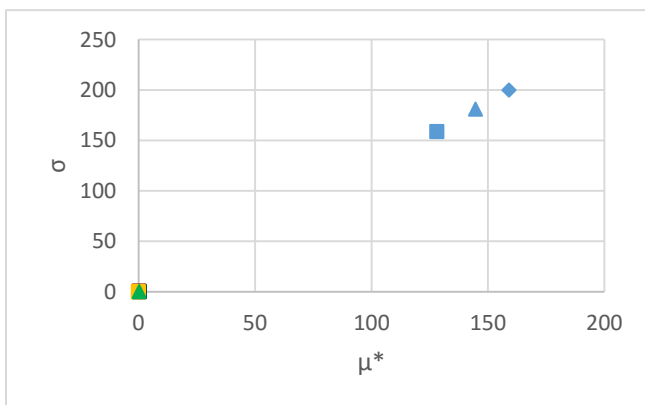


Figure C.5.4: CFAST results. Temperature exit 1

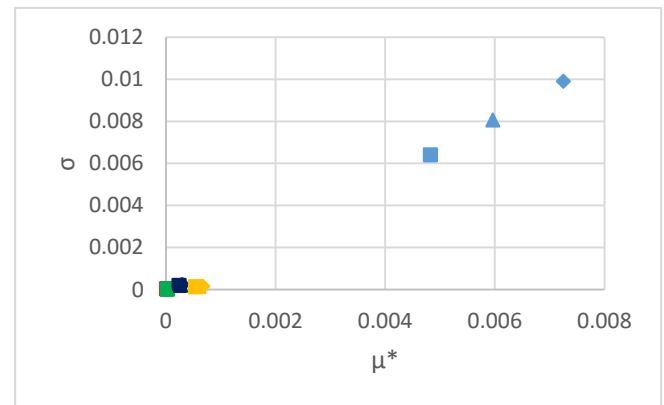


Figure C.5.3: CFAST results. CO levels exit 1 upper layer

**C.6. Total sensitivity index results bar with sprinkler system at exit 1 tables C.6.1 – C.6.2:**

<b>Output</b>	<b>St <math>\alpha</math> %</b>	<b>St HRRPUA %</b>	<b>St Area %</b>	<b>St HOC %</b>	<b>St CO %</b>
Temperature	81.79%	0.00%	15.56%	1.43%	1.21%
CO levels	22.39%	0.00%	1.39%	3.30%	72.93%

**Table C.6.1: FDS results. Total sensitivity index exit 1**

<b>Output</b>	<b>St <math>\alpha</math> %</b>	<b>St HRRPUA %</b>	<b>St Area %</b>	<b>St HOC %</b>	<b>St CO %</b>
Temperature	99.71%	0.07%	0.16%	0.06%	0.00%
CO levels upper layer	16.61%	0.04%	0.14%	4.41%	78.81%

**Table C.6.2: CFAST results. Total sensitivity index exit 1**



**C.7. Resulting  $\mu^*$  and  $\sigma$  bar with extraction system at exit 1 shown in figures C.7.1 – C.7.4:**

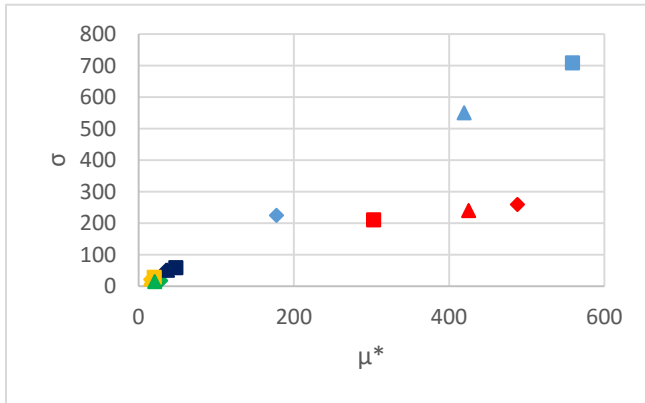


**Figure C.7.1: FDS results. Temperature exit 1**

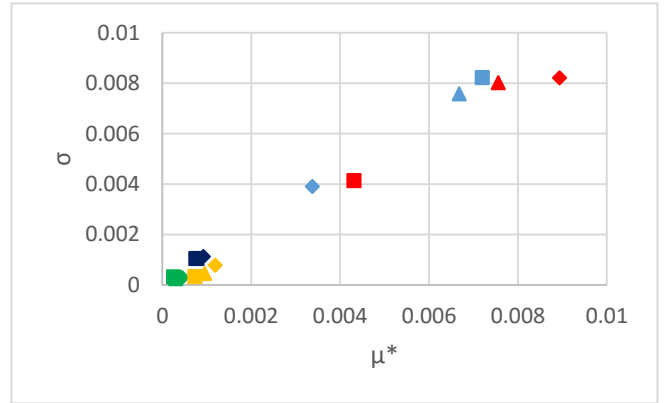


**Figure C.7.2: FDS results. CO levels exit 1**

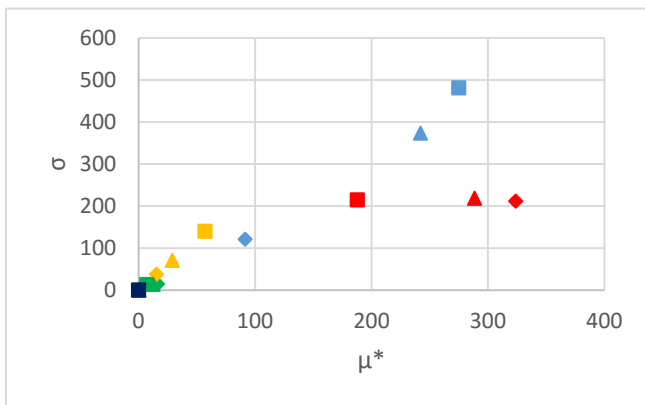


**Figure C.7.3: CFAST results. Temperature exit 1**

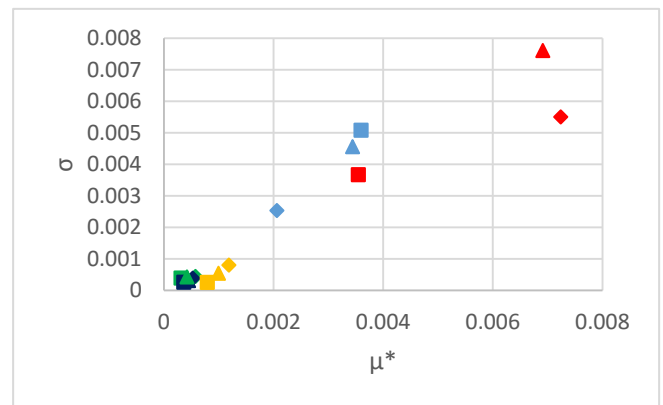


**Figure C.7.4: CFAST results. CO levels exit 1 upper layer**

**C.8. Total sensitivity index results bar with extraction system at exit 1 tables C.8.1 – C.8.2:**

Output	St $\alpha$ %	St HRRPUA %	St Area %	St HOC %	St CO %
Temperature	5.69%	91.90%	1.49%	0.35%	0.57%
CO levels	3.39%	91.61%	0.61%	0.88%	3.51%

**Table C.8.1: FDS results. Total sensitivity index exit 1**

Output	St $\alpha$ %	St HRRPUA %	St Area %	St HOC %	St CO %
Temperature	7.12%	88.15%	0.85%	0.00%	3.88%
CO levels upper layer	2.21%	90.43%	0.91%	1.22%	5.23%

Table C.8.2: CFAST results. Total sensitivity index exit 1

**C.9. Resulting  $\mu^*$  and  $\sigma$  bar ventilation-controlled fire exit 1 shown in figures C.9.1 – C.9.4:**

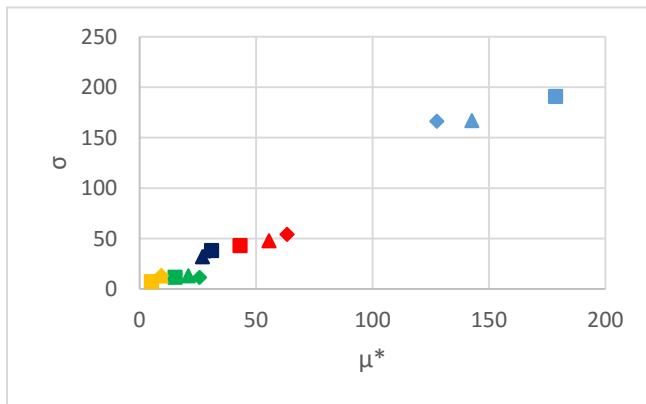


Figure C.9.1: FDS results. Temperature exit 1

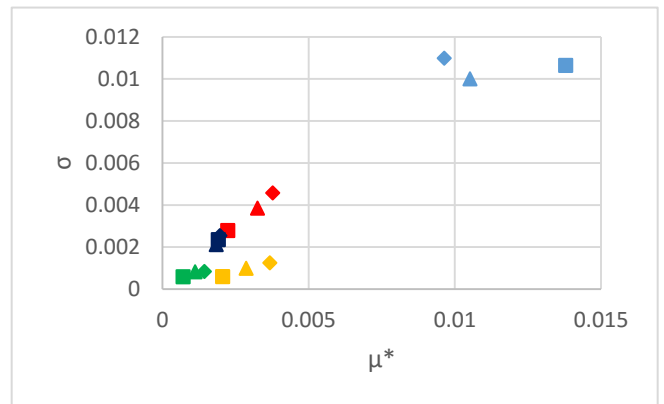


Figure C.9.2: FDS results. CO levels exit 1

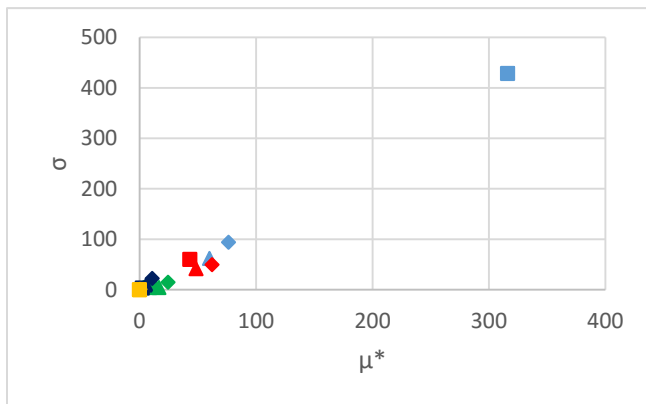


Figure C.9.3: CFAST results. Temperature exit 1

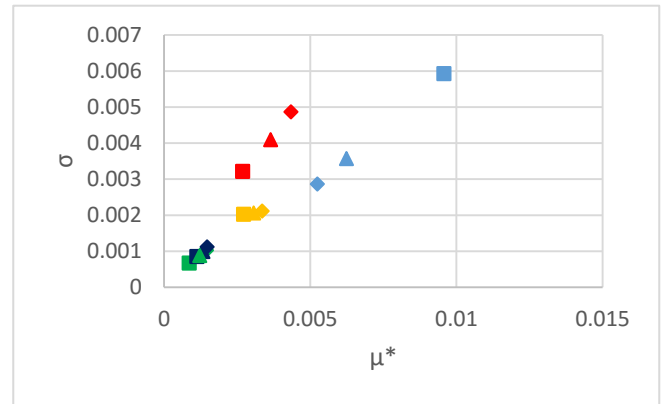


Figure C.9.4: CFAST results. CO levels exit 1 upper layer

**C.10. Total sensitivity index results bar ventilation-controlled fire exit 1 tables C.10.1 – C.10.2:**

Output	St $\alpha$ %	St HRRPUA %	St Area %	St HOC %	St CO %
Temperature	8.61%	57.72%	20.99%	10.37%	2.31%

CO levels	8.01%	20.71%	7.97%	5.98%	57.33%
-----------	-------	--------	-------	-------	--------

**Table C.10.1: FDS results. Total sensitivity index exit 1**

<b>Output</b>	<b>St <math>\alpha</math> %</b>	<b>St HRRPUA %</b>	<b>St Area %</b>	<b>St HOC %</b>	<b>St CO %</b>
Temperature	20.83%	47.16%	13.58%	18.43%	0.00%
CO levels	3.07%	20.40%	7.16%	5.21%	64.17%

**Table C.10. 2: CFAST results. Total sensitivity index exit 1**